Chemistry & Biology
Article

Activators of Cylindrical Proteases as Antimicrobials: Identification and Development of Small Molecule Activators of ClpP Protease

Elisa Leung,[1] Alessandro Datti,[2,3] Michele Cossette,[4] Jordan Goodreid,[4] Shannon E. McCaw,[5] Michelle Mah,[5] Alina Nakhamchik,[5] Koji Ogata,[6,11] Majida El Bakkouri,[1] Yi-Qiang Cheng,[7] Shoshana J. Wodak,[5,6,8] Bryan T. Eger,[1,5,9,10] Emil F. Pai,[1,5,9,10] Jun Liu,[5] Scott Gray-Owen,[5] Robert A. Batey,[4] and Walid A. Houry[1,*]

[1]Department of Biochemistry, University of Toronto, Toronto, ON M5S 1A8, Canada
[2]Samuel Lunenfeld Research Institute, Mount Sinai Hospital, Toronto, ON M5G 1X5, Canada
[3]Department of Experimental Medicine and Biochemical Sciences, University of Perugia, Perugia 06126, Italy
[4]Department of Chemistry
[5]Department of Molecular Genetics
University of Toronto, Toronto, ON M5S 1A8, Canada
[6]Centre for Computational Biology, Hospital for Sick Children, 555 University Avenue, Toronto, ON M5G 1X8, Canada
[7]Department of Biological Sciences and Department of Chemistry and Biochemistry, University of Wisconsin–Milwaukee, Milwaukee, WI 53211, USA
[8]Molecular Structure and Function Program, Hospital for Sick Children, 555 University Avenue, Toronto, ON M5G 1X8, Canada
[9]Department of Medical Biophysics, University of Toronto, Toronto, ON M5S 1A8, Canada
[10]Division of Cancer Genomics and Proteomics, Ontario Cancer Institute/Princess Margaret Hospital, Campbell Family Institute for Cancer Research, Toronto, ON M5G 1L7, Canada
[11]Present address: RIKEN, Innovation Center, 2-1 Hirosawa, Wako, Saitama 351-0198, Japan
*Correspondence: walid.houry@utoronto.ca
DOI 10.1016/j.chembiol.2011.07.023

SUMMARY

ClpP is a cylindrical serine protease whose ability to degrade proteins is regulated by the unfoldase ATP-dependent chaperones. ClpP on its own can only degrade small peptides. Here, we used ClpP as a target in a high-throughput screen for compounds, which activate the protease and allow it to degrade larger proteins, hence, abolishing the specificity arising from the ATP-dependent chaperones. Our screen resulted in five distinct compounds, which we designate as Activators of Self-Compartmentalizing Proteases 1 to 5 (ACP1 to 5). The compounds are found to stabilize the ClpP double-ring structure. The ACP1 chemical structure was considered to have drug-like characteristics and was further optimized to give analogs with bactericidal activity. Hence, the ACPs represent classes of compounds that can activate ClpP and that can be developed as potential novel antibiotics.

INTRODUCTION

In recent years, there has been an alarming trend of increased bacterial infections caused by strains resistant to most known antibiotics. As a result, diseases that were thought to be controlled by currently available drugs are re-emerging not only in developing countries but also in industrialized nations, especially in clinical settings such as hospitals. Therefore, there is an urgent need for the development of new types of antibiotics that can be used to effectively treat multidrug-resistant bacteria. The development of new drugs with novel mechanisms of action is clearly needed to avert an impending crisis.

Recently, a novel antibacterial target was identified when Brötz-Oesterhelt et al. (2005) discovered that the caseinolytic protease P, ClpP, is activated by acyldepsipeptides, ADEPs, a class of compounds that were first reported to have antibiotic properties in 1985 (Michel and Kastner, 1985). The ADEPs were later chemically optimized to address issues related to potency and aqueous solubility (Hinzen et al., 2006). The protein target of the ADEPs, ClpP protease, is a tetradecameric serine protease comprised of two stacked heptameric rings, which, in *Escherichia coli*, can form complexes with the AAA+ ATPase chaperones ClpX or ClpA (Katayama et al., 1988; Maurizi and Xia, 2004). ClpX and ClpA are hexameric chaperones that bind on one or both ends of the ClpP protease. The chaperones bind to target proteins, unfold them, and then thread them into the ClpP proteolytic chamber through axial pores lined by axial loops for degradation. These activities require ATP (Gottesman et al., 1997). In the absence of the ATPase components, ClpP alone can efficiently degrade small peptides of up to about 30 amino acids (Gottesman et al., 1997) and can also degrade unstructured proteins albeit with much lower efficiency when compared with ClpXP or ClpAP (Jennings et al., 2008; Bewley et al., 2009). ADEPs enhance the efficiency of ClpP-dependent degradation of unstructured proteins by opening up the ClpP axial pores (Lee et al., 2010; Li et al., 2010).

The aforementioned studies demonstrated that ClpP is an attractive target for developing new antibiotics with a novel mode of action. In this study, we have identified, by using a high-throughput screening approach, several structurally

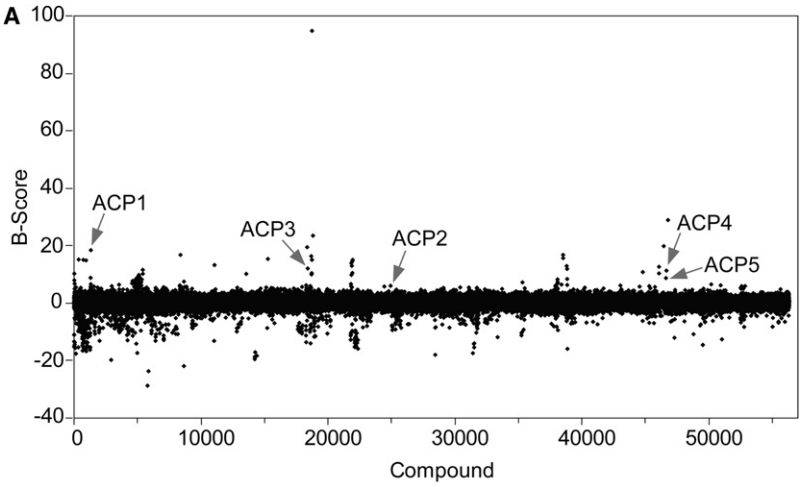

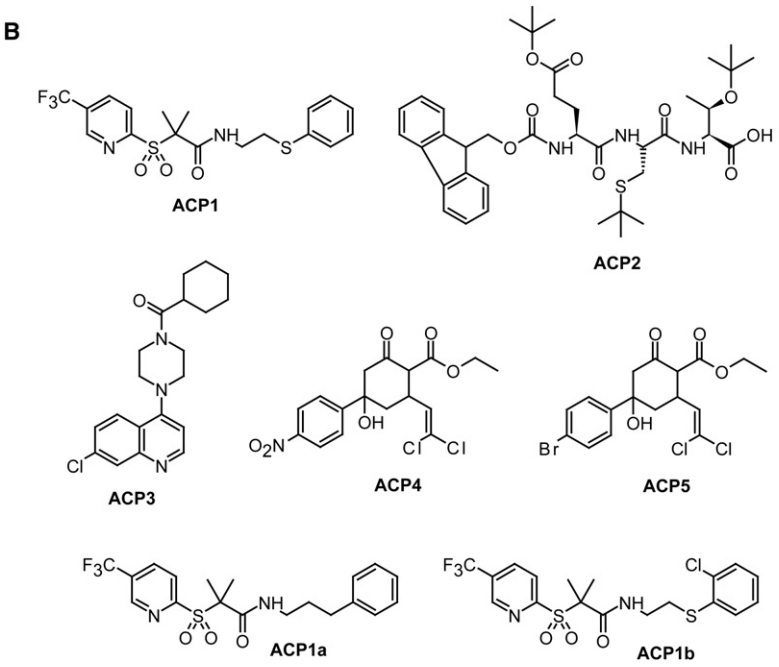

Figure 1. Results of the High-Throughput Compound Screen for Activators of ClpP

(A) About 60,000 compounds were screened to find activators of *E. coli* ClpP. B-score values were calculated for each compound from the increase in fluorescence intensity after a 6 hour incubation of casein-FITC with ClpP and compound. Compounds confirmed as hits, designated ACP1 through ACP5, are indicated by the arrows (see also Figure S1). Other compounds with high B-scores were false hits.

(B) Shown are chemical structures of ACP1-ACP5 as well as of ACP1a and ACP1b. ACP1 is N-1-[2-(phenylthio) ethyl]-2-methyl-2-{[5-(trifluoromethyl)-2-pyridyl]sulfonyl}propanamide, ACP2 is 3-(tertbutoxy)-2-{[2-[(5-(tertbutoxy)-2-{[(9-H-9-fluorenylmethoxy)carbonyl]amino}-5-oxopentanoyl) amino]-3-(tertbutylsulfanyl)propanoyl]amino}butanoic acid, ACP3 is [4-(7-chloroquinolin-4-yl)piperazino](cyclohexyl) methanone, ACP4 is ethyl 2-(2,2-dichlorovinyl)-4-hydroxy-4-(3-nitrophenyl)-6-oxocyclohexanecarboxylate, and ACP5 is ethyl 4-(4-bromophenyl)-2-(2,2-dichlorovinyl)-4-hydroxy-6-oxocyclohexanecarboxylate.

diverse non-ADEP compounds that activate the ClpP proteolytic core to degrade protein substrates in the absence of the ClpX or ClpA ATPases. These newly identified compounds have been termed Activators of Self-Compartmentalizing Proteases (ACP). Their chemical structures differ significantly from the structures of the previously identified ADEPs. The chemical optimization of ACP1 resulted in analogs having improved bioactivity and bactericidal effects. Hence, our study provides the basis for the development of novel antibiotics based on the activation and dysregulation of ClpP activity using different structural scaffolds.

RESULTS

High-Throughput Screen for ClpP Activators

To identify compounds that activate ClpP, we developed a high-throughput screening assay with a fluorescence-based readout. The assay employed fluorescein isothiocyanate-labeled casein (casein-FITC) as the proteolytic target of the *E. coli* ClpP protease. When casein-FITC is intact, FITC fluorescence is quenched; protease-catalyzed hydrolysis of casein-FITC relieves this quenching, yielding highly fluorescent dye-labeled peptides. The principle of the screen was to select for compounds that result in increased fluorescence upon incubation of casein-FITC with ClpP. Preliminary tests performed in the presence and absence of the unfoldase chaperone ClpA revealed a 5-fold dynamic range after 30 min incubation and intra- and interassay variability, expressed as coefficient of variation, of 2% and 5%, respectively. In light of ClpP stability over several hours at 37°C, reactions were typically monitored every 15 min for 6 hr to rule out time-dependent effects.

With the initial intent of exploring drug-repositioning opportunities, we employed 4500 chemicals composed of biologically and pharmacologically active entities, of which approximately 45% were marketed drugs or drug candidates evaluated in clinical trial stages. Notably, none of these compounds were active at a concentration of 10 μM, suggesting the necessity to significantly broaden chemical diversity to explore ClpP druggability and the likelihood to activate ClpP using small molecules. Thus, we expanded the screening campaign to include additional ~60,000 highly diverse, drug-like chemicals. This undertaking was carried out using a final compound concentration of 20 μM. Results were normalized and corrected for systematic errors using the B-score method (Brideau et al., 2003) (Figure 1A) and positive hits were defined as the compounds whose signals were at least three standard deviations (99.73% confidence interval) from the mean of the general sample population. An excellent quality of the screening setup was shown by the dimensionless parameters Z′- and Z-factors (Zhang et al.,

A

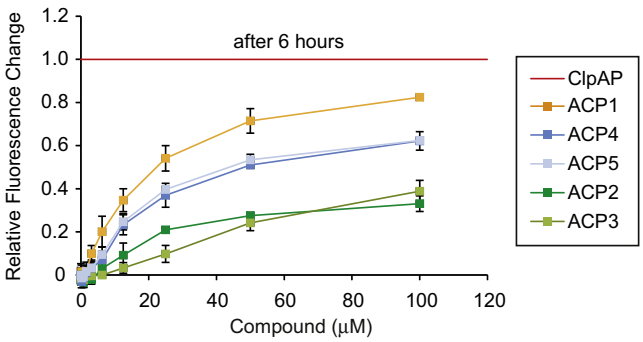

B

Compound	RD25	SD
ACP1	0.53	0.04
ACP2	0.20	0.01
ACP3	0.10	0.04
ACP4	0.37	0.05
ACP5	0.39	0.04

Figure 2. Relative Degradation Index

(A) Shown is the effect of compound concentration on casein-FITC degradation by ClpP after 6 hour incubation. Data are the average of three repeats. Error bars represent standard deviations.

(B) Comparison of the RD25 values for the ACP compounds. Data shown represent the average of three repeats. SD is standard deviation.

1999), which were consistently in the 0.7 range throughout the entire screening campaign, thereby, indicating an effective combination of dynamic range, variability, and hit rate.

This chemical screen led to the selection of five confirmed hits (Figure 1B), that were designated ACP1 to 5. ACP1, ACP2, and ACP3 were hits from the Maybridge library, while ACP4 and ACP5 were hits from the Chembridge library. Interestingly, ACP4 and ACP5 were analogous molecules, with identical structures that only differed in the modification of an aromatic group (Figure 1B).

Characterization of ACP-Mediated ClpP Activation

To assess and compare the potency of ACPs, dose-response analyses were carried out following the degradation of casein-FITC for 6 hours (Figure 2A). The results were evaluated using a quantitative measure, which we developed and named the relative degradation index (RD), defined as follows:

$$\mathbf{RD} = \frac{\left(\Delta\varphi_{\mathrm{ClpP+compound}}\right)_{\text{after 6 hrs}} - \left(\Delta\varphi_{\mathrm{ClpP}}\right)_{\text{after 6 hrs}}}{\left(\Delta\varphi_{\textit{E.coli}\ \mathrm{ClpAP}}\right)_{\text{after 6 hrs}} - \left(\Delta\varphi_{\textit{E.coli}\ \mathrm{ClpP}}\right)_{\text{after 6 hrs}}}. \quad (1)$$

$\Delta\varphi$ is the change in fluorescence after 6 hr of starting the reaction (see Experimental Procedures) measured using 485 nm excitation and 535 nm emission, which primarily detects the signal from casein-FITC. *E. coli* ClpAP was used as a benchmark for maximum ClpP proteolytic activity. The ClpP in the numerator can be from any other organism. Based on RD25 measurements, which refers to the measurement in the presence of 25 μM compound, the ranking of the activators from strongest to weakest is as follows: ACP1, ACP5, ACP4, ACP2, and ACP3 (Figure 2B). It should be emphasized that the RD value reflects how much casein is degraded after 6 hr and, in theory, need not directly correlate with the K_d for the binding of a given compound to casein or with degradation rates, although, in practice, we observe a general correspondence between these parameters.

The activation of ClpP by the various ACPs was further confirmed by direct observation of unlabeled casein degradation on SDS-PAGE gels (see Figure S1A available online), which also indicated that the rank order of compound-mediated ClpP activation was consistent with the observations obtained from fluorometric determinations.

In order to verify that the activators were acting on ClpP rather than on the casein substrate directly, the ability of compound-activated ClpP to degrade proteins from various organisms was tested using a variety of model substrates and unrelated proteins (Figures S1B and S1C). The stronger activators induced ClpP to degrade a wider variety of protein substrates than the weaker activators with no apparent specificity. However, the proteins subject to extensive proteolytic cleavage, such as Casein (Creamer et al., 1981), Tah1 (Zhao et al., 2005), CFTR R-region (Ostedgaard et al., 2001), reduced carboxymethylated α-lactalbumin (RCMLa), λN protein (Mogridge et al., 1998), and α-synuclein (Tompa, 2009) are either considered to be unstable or disordered proteins or to have disordered regions. Conversely, well-folded substrates, such as GFP-SsrA and creatine kinase, were degraded to a lesser extent or not at all, likely due to the stability of their structures. Proteins that were only clipped, but not completely degraded, by compound-activated ClpP (α-M protein, ClpA, and ClpX) were all larger sized proteins.

Chemical Optimization of ACP1

When tested for bactericidal properties against ten different bacteria, several of the ACPs showed minimum bactericidal concentrations (MBC in μg/ml) at relatively low concentrations (Table 1). Although certain compounds were more effective against some bacteria compared with others, it was generally observed that gram-negative bacteria were more sensitive to these compounds than gram-positives (Table 1).

To determine whether the effects observed were due to the interaction of the ACPs with ClpP in the bacteria, we constructed *N. meningitidis* H44/76 strain (Nme H44/76, a genetically tractable strain) in which the *clpP* gene was disrupted as described in Experimental Procedures. The disruption of *clpP* was verified by PCR (Figure S2A). The susceptibility of WT and Δ*clpP* Nme H44/76 strains to the different compounds was assessed using either the disk diffusion plate assay or the liquid culture MBC assay. A differential effect was observed for ADEP1A and ADEP1B (Figure S2B) in addition to ACP1 and, to a weaker extent, ACP4 (not shown). For ACP1, the MBC for WT Nme H44/76 was 128 μg/ml, while for Δ*clpP* it was 64 μg/ml. The Nme H44/76 Δ*clpP* strain was more resistant to the effect of the compounds compared with WT as would be expected if the compounds are primarily targeting the bacterial ClpP. These observations prompted us to implement medicinal chemistry rationales aimed at the refinement and optimization of primary hits.

The chemical structures of ACP1–5 (Figure 1B) do not show any obvious structural similarities with each other, except for ACP4 and 5, or with the ADEPs (Figure S2C). ACP4 and 5 were considered to be unsuitable for further optimization as they do

Table 1. Minimum Bactericidal Concentration of Compounds

	ADEP1A		ACP1		ACP2		ACP3		ACP4		ACP5		ACP1a		ACP1b	
PMBN	+	–	+	–	+	–	+	–	+	–	+	–	+	–	+	–
N. gonorrhoeae (N.279)	0.125[a]	0.125[a]	>256	>256	32[b]	32[b]	>256	>256	4[a]	4[a]	>256	>256	128	>256	>256	>256
N. meningitidis (MC58)	0.25[a]	0.25[a]	64[b]	64[b]	>256	64[b]	>256	>256	32[b]	32[b]	>256	>256	64[b]	64[b]	16[b]	16[b]
H. influenzae (H2192)	8[a]	128	64[b]	>256	8[a]	>256	>256	>256	4[a]	128	32[b]	>256	32[b]	>256	8[a]	>256
E. coli (DH5α)	16[b]	>256	>256	>256	8[a]	>256	>256	>256	16[b]	>256	16[b]	>256	>256	>256	>256	>256
S. typhimurium (SL1344)	>256	>256	>256	>256	>256	>256	>256	>256	>256	>256	>256	>256	>256	>256	>256	>256
P. aeruginosa (PAO1)	16[b]	>256	>256	>256	8[a]	>256	>256	>256	>256	>256	>256	>256	>256	>256	>256	>256
S. aureus (ATCC 29213)	N/A	4[a]	N/A	>256	N/A	>256	N/A	>256	N/A	>256	N/A	>256	N/A	>256	N/A	>256
S. pneumoniae (ATCC 49619)	N/A	16[b]	N/A	>256	N/A	16[b]	N/A	>256	N/A	8[a]	N/A	>256	N/A	N/A	N/A	N/A
L. monocytogenes (EGD)	N/A	0.125[a]	N/A	>256	N/A	32[b]	N/A	>256	N/A	>256	N/A	>256	N/A	N/A	N/A	N/A
M. smegmatis (mc^2155)	N/A	>256	N/A	>256	N/A	>256	N/A	>256	N/A	128	N/A	256	N/A	>256	N/A	>256

128 or more except where indicated with a footnote. The membrane permeabilizing agent polymyxin B nonapeptide, PMBN, was added at 120 μg/ml where indicated.
[a] 0.125–8.
[b] 16–64.

not have drug-like structures and would be more challenging to assess in a structure activity relationship (SAR) studies (Keller et al., 2006). ACP2 would be relatively straightforward to evaluate in an SAR study, but the protected tripeptide derivative framework was not considered optimal as a potential small-molecule lead. Instead, ACP1 and 3 both display drug-like structures amenable to further optimization, synthesis, and SAR studies. In light of the higher RD25 score for ACP1 (Figure 2B) and the fact that it seems to indeed target ClpP in the cell as described above, we decided to explore chemical diversity around the ACP1 molecule.

ACP1 satisfies Lipinski's rule of five (Lipinski et al., 2001) and has a topological polar surface area of 75.6, calculated molar refractivity of 10.4, and Clog P of 3.98. The structure of ACP1 consists of a central β-amido sulfone core appended with a western electron deficient pyridyl ring and an eastern hydrophobic tail incorporating a phenylthioether group (Figures 1B and 3A). The natural synthetic disconnection point chosen for the synthesis of ACP1 analogs was the amide linkage (Figure 3A). Analogs were synthesized using a late-stage amide-bond forming reaction between the eastern amine and the western β-sulfonyl carboxylic acid (Figure 3B) by applying standard synthetic protocols (see Experimental Procedures) and, subsequently, evaluated by measuring their RD25 values. We used the natural products ADEP1 factor A and B (Figure S2C) isolated from *Streptomyces hawaiiensis* (see Experimental Procedures) as a reference. ADEP1A is a better ClpP activator than ADEP1B (Figure 3C).

Of more than 70 analogs generated, one compound, which we termed ACP1b (Figure 1B), was found to exhibit an RD25 value slightly higher than that of ADEP1A (Figure 3C). For comparison, another analog, which we termed ACP1a (shown in Figure 1B), displayed a lower RD25 value than that of ACP1b but comparable to that of ADEP1B (Figure 3C). ACP1a incorporates a sulfur to methylene substitution in the eastern tail, and ACP1b has an *ortho*-chloro substituent in the arylthioether ring (Figure 1B).

The extent of casein degradation upon activation of ClpP by these compounds is shown in Figure 3D and is generally consistent with the RD25 results. It has previously been shown that ADEPs activate *E. coli* ClpP to degrade casein with reduced processivity (Brötz-Oesterhelt et al., 2005; Kirstein et al., 2009). This was also true for ACP1, ACP1a, and ACP1b (Figure 3E). The patterns of appearance and disappearance of the degradation intermediates suggests similarities between the general mechanisms of activation by the different compounds.

Notably, among the different bacterial species tested, ACP1b showed an MBC value against *H. influenzae* that was comparable to that of ADEP1A and much lower than that of ACP1 and ACP1a (Table 1). ACP1b also had improved MBC value against *N. meningitidis* MC58 compared with ACP1 and ACP1a, but not ADEP1A (Table 1). The MBC values for ACP1b were 32 and 64 μg/ml for WT and Δ*clpP* Nme H44/76 described above, respectively. Hence, while the WT is more sensitive to ACP1b than the Δ*clpP* strain indicating that ClpP is indeed a target for the compound in the cell, ACP1b might have other cellular targets and further optimization will have to concentrate on increasing specificity.

Although ACP1b was optimized against *E. coli* ClpP, *E. coli* DH5α was resistant to this compound (Table 1), which is consistent with earlier results (Brötz-Oesterhelt et al., 2005).

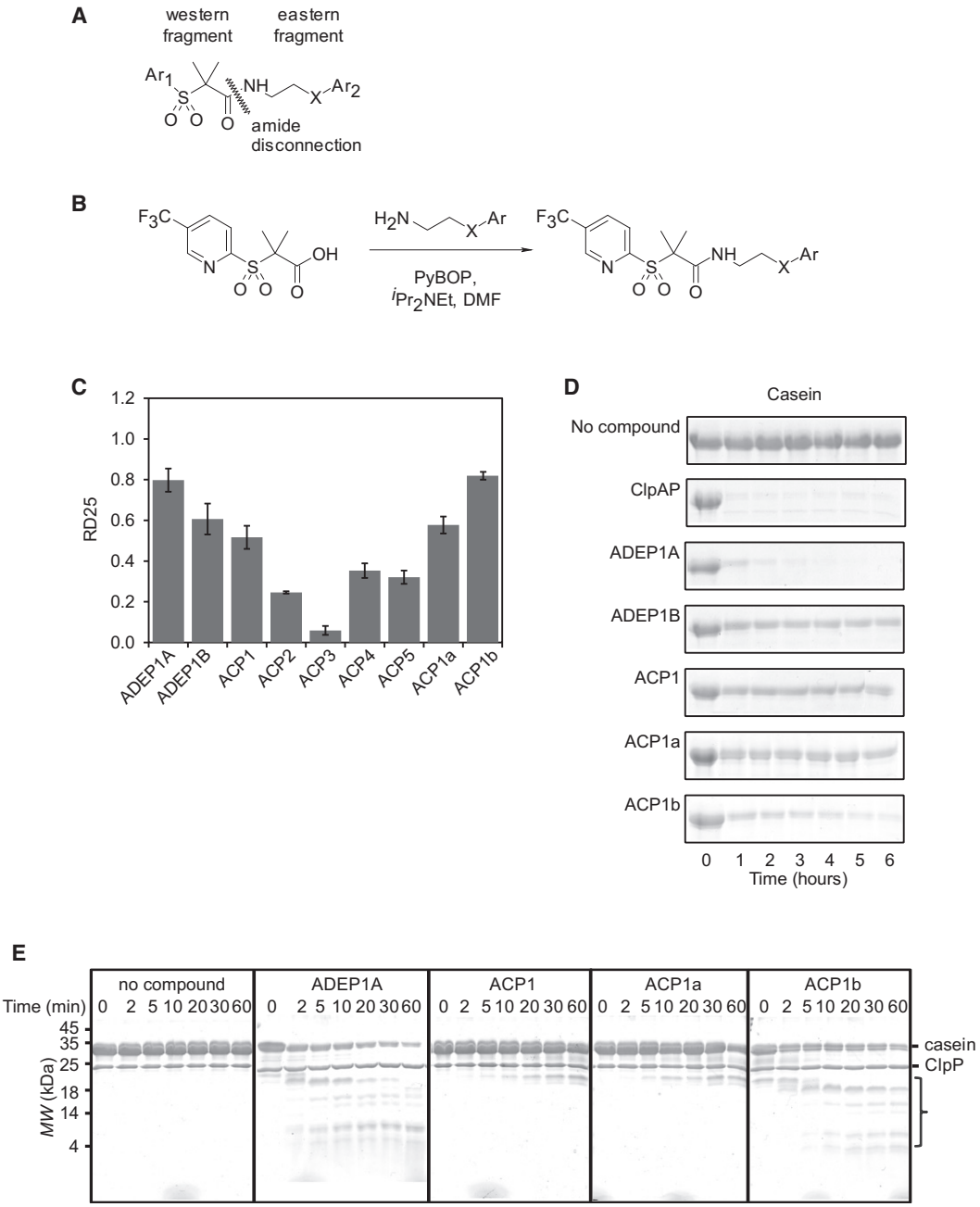

Figure 3. Chemical Optimization of ACP1

(A) General chemical structure of the ACP1 analogs.

(B) A schematic of the chemical reaction to synthesize the ACP1 analogs using PyBoP mediated amide bond formation between 2-methyl-2-((5-(trifluoromethyl) pyridin-2-yl)thio)propanoic acid and primary amines.

(C) RD25 values of ADEP1A, ADEP1B, ACP1–5, ACP1a, and ACP1b (see also Figure S2). Error bars represent the standard deviations from the average of three repeats.

(D) Shown is the degradation of unlabeled casein by compound-activated ClpP followed on SDS-PAGE gels.

(E) The formation of intermediates during casein degradation by compound-activated ClpP.

Intermediate species, indicated by the parenthesis, resulting from casein degradation were resolved on 18% SDS-PAGE gels.

Brötz-Oesterhelt et al. (2005) did not see an effect of ADEPs on WT *E. coli*, but rather on an *E. coli* strain deleted of the multidrug efflux pump AcrA in the presence of the outer membrane permeabilizer polymyxin B nonapeptide (PMBN). Hence, we combined ACP1b with several other known drugs to enhance sensitivity. Using this approach, ACP1b was found to affect cell growth of *E. coli* MC4100 strain in the presence of 20 μM of the uncoupler ionophore carbonyl cyanide 3-chlorophenylhydrazone (CCCP)

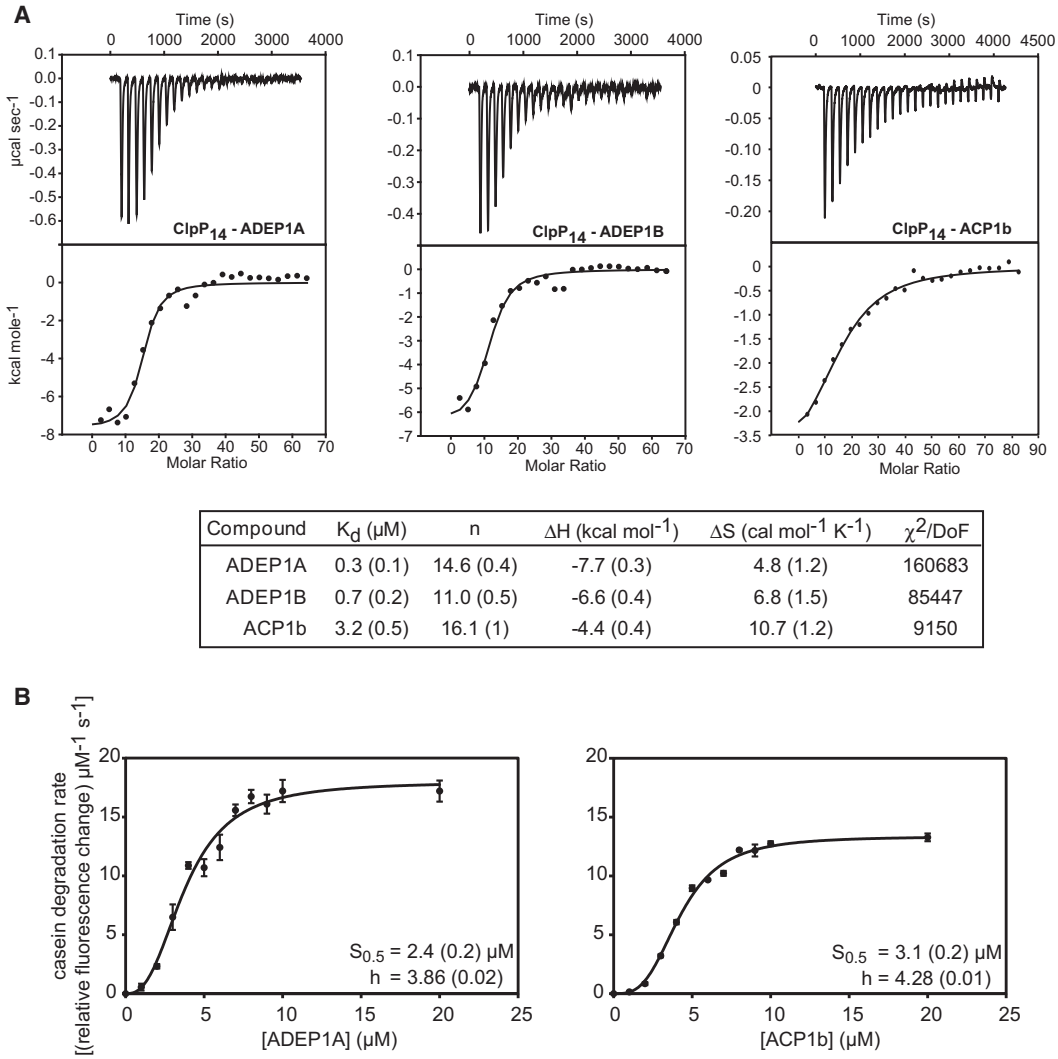

Compound	K_d (μM)	n	ΔH (kcal mol^{-1})	ΔS (cal mol^{-1} K^{-1})	χ^2/DoF
ADEP1A	0.3 (0.1)	14.6 (0.4)	-7.7 (0.3)	4.8 (1.2)	160683
ADEP1B	0.7 (0.2)	11.0 (0.5)	-6.6 (0.4)	6.8 (1.5)	85447
ACP1b	3.2 (0.5)	16.1 (1)	-4.4 (0.4)	10.7 (1.2)	9150

Figure 4. Determination of Binding Affinity of Compounds to ClpP

(A) ITC binding curves for ClpP-ADEP1A, ADEP1B, or ACP1b interaction are shown. Results for the fit of the data to a one set of identical independent binding site model is given in the table. Numbers in parentheses refer to standard deviations. χ^2/DoF refers to chi-square divided by the degrees of freedom and indicates the quality of the fit (see also Figure S3).

(B) Cooperativity of binding of ADEP1A and ACP1b to ClpP was determined by measuring the change in casein degradation rate by compound-activated ClpP as a function of compound concentration. Error bars represent the standard deviations from the average of three repeats.

(Figure S2D). This sensitivity was not observed for MC4100 Δ*clpP* strain consistent with ClpP being a target for ACP1B in the cell.

The above observations indicate that the antibacterial properties of ACP1 can be improved through relatively simple chemical modifications and that further efforts will have to concentrate on enhancing specificity.

Determination of Binding Affinity and Stoichiometry of ACP1b Interaction with ClpP

The dissociation constant (K_d) for the binding of ACP1b to ClpP was measured using isothermal titration calorimetry (ITC) and was found to be about 3.2 ± 0.5 μM, which is comparable to, albeit slightly higher, than that of ADEP1A (0.3 ± 0.1 μM) and ADEP1B (0.7 ± 0.2 μM) (Figure 4A). The ITC data were fit by allowing the number of binding sites (n) to vary (Figure 4A), by fixing n to a whole number (Figure S3A), or by fixing n to 14 (Figure S3B). The results suggest that there are 14 binding sites for the ADEPs and ACP1b on $ClpP_{14}$. In comparison, ACP1 has a dissociation constant for ClpP of about 130 μM as determined by Surface Plasmon Resonance (SPR) measurements (Figure S3C), whereas ITC was unsuitable to measure ACP1 affinity for ClpP due to weak binding. The similar K_d values obtained for the ADEPs by SPR (Figure S3C) and ITC (Figure 4A) clearly indicate that ACP1 has lower affinity than the ADEPs for ClpP. SPR experiments were also carried out for ACP2–5, and the K_d values obtained were much weaker (>150 μM) than that of ACP1 as expected (data not shown).

Measurement of casein degradation rate by compound-activated ClpP as a function of ADEP1A or ACP1b concentration resulted in a sigmoidal saturation curve with $S_{0.5}$ of 2–3 μM and

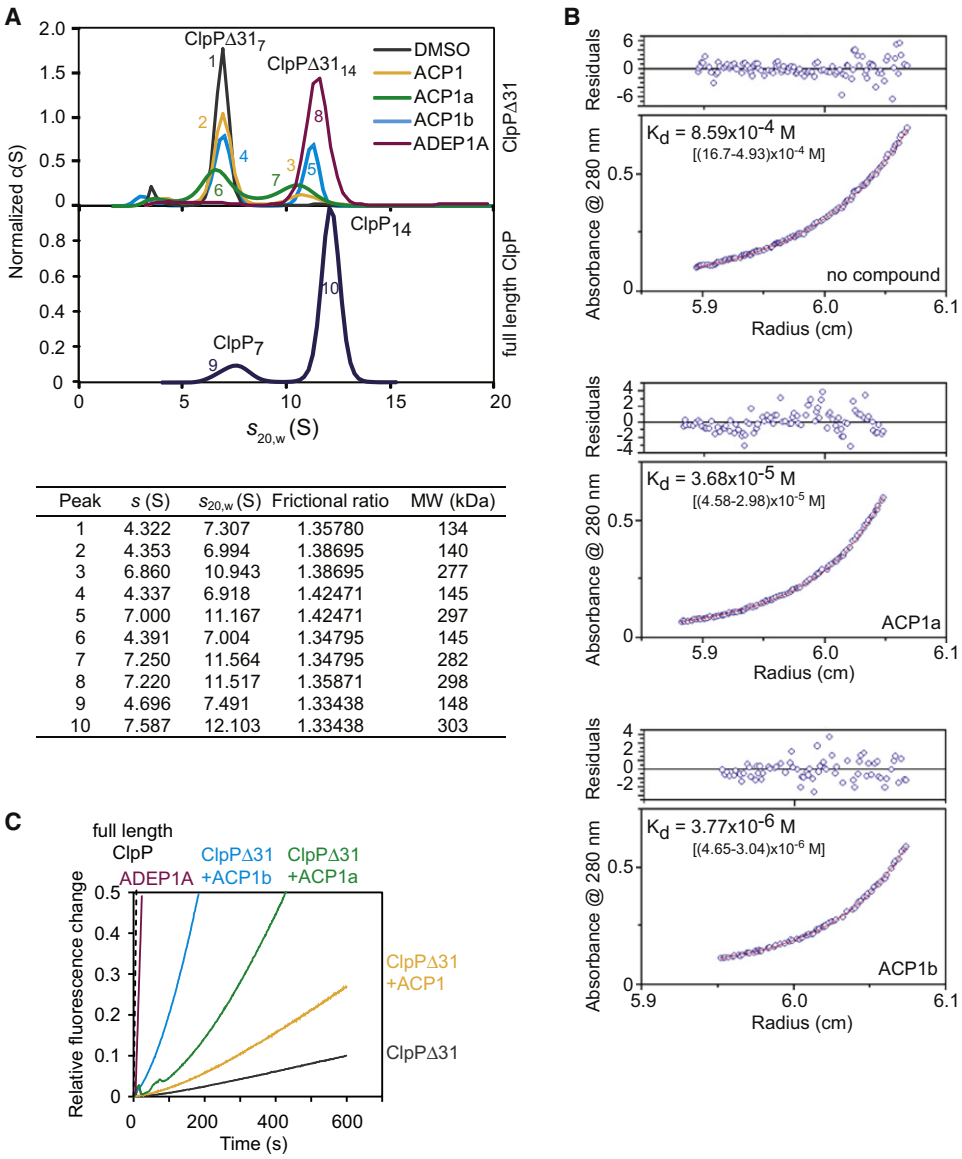

Peak	s (S)	$s_{20,w}$ (S)	Frictional ratio	MW (kDa)
1	4.322	7.307	1.35780	134
2	4.353	6.994	1.38695	140
3	6.860	10.943	1.38695	277
4	4.337	6.918	1.42471	145
5	7.000	11.167	1.42471	297
6	4.391	7.004	1.34795	145
7	7.250	11.564	1.34795	282
8	7.220	11.517	1.35871	298
9	4.696	7.491	1.33438	148
10	7.587	12.103	1.33438	303

Figure 5. Effect of ACP on ClpP Oligomeric Stability

(A) Sedimentation velocity analytical ultracentrifugation of full length ClpP (46 μM) and ClpPΔ31 (51 μM) at 4°C shown using the continuous distribution model c(S) versus $s_{20,w}$, scaled to initial absorbance. ACP1, ACP1a, ACP1b, and ADEP1A (at 100 μM) promote the tetradecamerization of ClpPΔ31 to different extents. The table lists the sedimentation coefficients, frictional ratios, and molecular weights corresponding to the various peaks.

(B) Sedimentation equilibrium profiles and the corresponding distribution of residuals for 51 μM ClpPΔ31 in the absence of compound (top), or in the presence of 100 μM ACP1a (middle) or 100 μM ACP1b (bottom). The solid lines represent the best fit to a monomer-dimer model, with the heptameric ClpP (MW of 138,544 Da) treated as the monomer. The resulting dissociation constants are given for each data set. The numbers in brackets give the range of K_d values for the 95% confidence interval.

(C) The effect of compounds (at 100 μM) on the peptidase activity of ClpPΔ31 (1 μM) is shown. The defective peptidase activity of this mutant is partially recovered by the presence of the ACP compounds.

a Hill coefficient, h, of about 4 (Figure 4B). The data suggest that these compounds act on ClpP in a similar manner and bind to the protease cooperatively or promote cooperative allosteric transitions within the protease structure.

The ClpP Tetradecamer Is Stabilized by ACP Binding

Thermal melt experiments indicated that the ACP compounds enhanced ClpP stability (not shown). Hence, we asked whether the compounds affect ring-ring interactions within the ClpP double-ring tetradecamer. An N-terminal truncation mutant of *E. coli* ClpP was originally constructed to open the central pore of the protease in an attempt to mimic a proposed mechanism of compound activation. However, this mutant, ClpPΔ31, mainly eluted as a heptameric single ring upon size exclusion chromatography and had no significant peptidase activity. In order to verify the oligomeric state of this protein, we employed sedimentation velocity analytical ultracentrifugation (Figure 5A). The results indicate that the ClpPΔ31 mutant has a sedimentation

coefficient corresponding to that of a heptamer; by comparison, WT ClpP has a sedimentation coefficient corresponding to a tetradecamer with a small proportion of heptamers (Figure 5A).

Addition of the different compounds shifts the oligomeric state of ClpPΔ31 to that of a tetradecamer (Figure 5A). The proportion of ClpPΔ31 tetradecamers formed correlates with the binding affinity of the compounds. For example, ACP1b led to the formation of a higher proportion of tetradecamers than ACP1, while ADEP1A led to the formation of the ClpPΔ31 tetradecamer exclusively. It should be noted that integration of the normalized c(S) signal over the s-values, which cover the range of sedimenting material, shows that the total "loading signal" is similar for the different curves with an average total loading signal of 0.52 (±0.12). The differences in the normalized c(S) peak heights is mainly because some peaks are broader than others for the various treatments of ClpPΔ31. Slight shifts in alignment of the ClpPΔ31 tetradecamer sedimentation coefficient in the presence of the various compounds might indicate some disassembly of the tetradecamer under the sedimentation velocity nonequilibrium conditions or may be attributed to different hydrodynamic properties of the tetradecamers formed. We further verified the oligomeric state of the ClpPΔ31 in the presence of ACP1a or ACP1b using sedimentation equilibrium experiments (Figure 5B). Fits of the data to monomer-dimer equilibrium, assuming the monomer is heptameric ClpPΔ31 with a molecular weight of 138,544 Da, clearly indicate that the presence of ACP1a or ACP1b decreases the dissociation constant of the ClpP tetradecamer with ACP1a having a lower K_d than ACP1b, which, in turn, is lower than that in the absence of the compound (Figure 5B).

Without the addition of compound, ClpPΔ31 had little protease activity (Figure 5C). Addition of ACP1, ACP1a, ACP1b, or ADEP1A promoted the formation of tetradecameric ClpPΔ31 (Figures 5A and 5B) and resulted in a catalytically active ClpPΔ31 (Figure 5C). These results strongly suggest that the ACP compounds stabilize ClpP by promoting the formation of the double-ring structure.

ACP Binding Sites on ClpP

The ADEPs have been found to bind in a hydrophobic pocket (H pocket) on the ClpP apical surface in which the IGF loop of the ClpX/ClpA ATPases also binds (Lee et al., 2010; Li et al., 2010). As a result, the presence of the ADEPs inhibited or reduced the ClpXP/ClpAP-mediated degradation of GFP-ssrA by interfering with the binding of ClpX/ClpA to ClpP. As shown in Figure 6A and Figure S4A, a similar effect was also seen for the ACPs suggesting that these compounds either bind to or allosterically modulate the H pocket of ClpP.

Two binding pockets on ClpP of equal probability were predicted by computational procedures implemented in DOCK6.3 software (Lang et al., 2009) (see Experimental Procedures; Figure 6B; Table S1), namely, the H pocket and a separate pocket, which we have named the C pocket, featuring a larger number of charged residues. The H pocket is composed of residues V42, F44, L62, Y74, Y76, I104, F126, L203, and R206 from one subunit, and L37 and F96 from the neighboring subunit (using Swiss-Prot numbering). The C pocket comprises residues Y90, M94, Q95, D100, V101, and H170 of one subunit and residues H205 and N207 of the neighboring subunit. Interestingly, the H and C pockets are separated by residues at the very C terminus of ClpP, corresponding to amino acids 203–207. While ADEPs cocrystallized with ClpP were found to be bound to the H pocket (Lee et al., 2010; Li et al., 2010), all the ACP compounds were docked well to both the H and C pockets (Figure 6B), and their docking scores differed little between the two pockets (Table S1).

To further validate the results of the docking analyses, we generated and tested mutants of the H pocket (Y76W [Lee et al., 2010], F126A [Bewley et al., 2006], and L203E), C pocket (Q95A, D100A, and H170A), as well as both the H and C pockets (Figure 6B). Peptidase assays were first performed to assess whether the mutations affected ClpP active sites. Except for Y76W, H170A, and Q95A/F126A, the mutants exhibited peptidase activity similar to that of the wild-type (WT) protein (Figure S4B). Intriguingly, we observed that the effects of stronger ClpP activators, such as ADEP1A and ACP1b, markedly decreased in the presence of mutations confined to the H pocket, whereas weaker activators appeared to be affected by mutations in both H and C pockets (Figure 6B). These findings, taken together, suggest that a successful strategy aimed at developing stronger ClpP activators is that of developing small molecules interacting with ClpP within the H pocket.

DISCUSSION

In our study, we have successfully identified five new compounds representing four different structural classes (Figure 1B) that activate ClpP protease and have bactericidal properties. With the exception of ACP4 and ACP5, these compounds have no apparent structural similarities to each other or to the previously reported ADEPs (Brötz-Oesterhelt et al., 2005), dramatically increasing the repertoire of compounds activating this protease. The optimization of ACP1 resulted in compounds that had in vitro ClpP activation properties close to that of the natural product ADEPs (Figure 3C). Importantly, these optimized compounds have good bactericidal properties (Table 1), suggesting potential applications as therapeutics. In particular, our data indicate that these compounds may be dramatically improved through a much tighter affinity for ClpP and specific targeting within the ClpP H pocket.

Based on the results of Figures 4–6, we propose that the identified ACP compounds share a similar mechanism of ClpP activation as the ADEPs. They all stabilize ClpP and promote the formation of the double-ring structure, albeit through a yet unknown mechanism. The apparent lack of substrate preference (Figures S1B and S1C) that the compounds confer on ClpP in addition to the similarities in degradation patterns (Figure 3E) is also indicative of similarities in mechanism of ClpP activation. The compounds prevent the binding of ClpP to its associated unfoldase (Figure 6A; Figure S4A) and, at the same time, activate nonspecific proteolysis probably through the opening of the axial pores.

The recently solved cocrystal structures of ADEP bound to *B. subtilis* and *E. coli* ClpP (Lee et al., 2010; Li et al., 2010) show ADEP binding to the H pocket of the protease. Our results are in general agreement with these findings; however, we propose the presence of an additional pocket, the C pocket, that is more charged (Figure 6B) and, as suggested by our

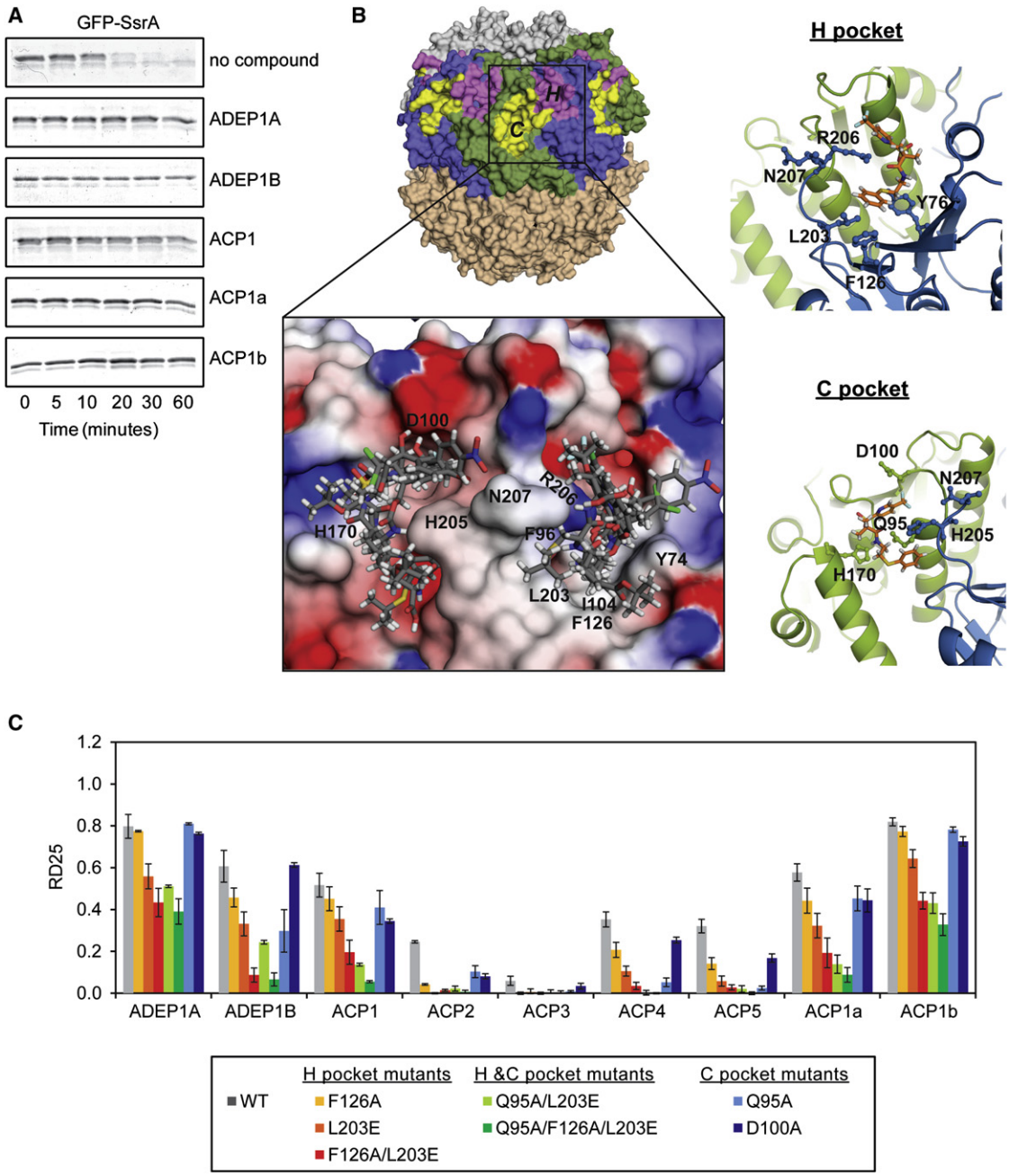

Figure 6. ACP Binding Sites

(A) Shown is the inhibition of ClpXP-mediated GFP-ssrA degradation by ACPs and ADEPs added at 100 μM monitored on SDS-PAGE gels. ClpP was preincubated with compound before the addition of ClpX (see also Figure S4A).

(B) Surface model of ClpP is shown on the top left. Four neighboring subunits are colored in alternating blue and green. The H pockets are colored in purple, while the C pockets are colored in yellow. The bottom left panel shows a close up view of the predicted compound binding conformations in the two ClpP pockets. The five ACP compounds are overlaid in the binding pockets (see also Table S1). ClpP is shown as a surface model and the compounds are shown as stick models. C, N, O, S, F, Cl, Br, and H in the compounds are colored in gray, blue, red, yellow, cyan, green, purple, and white, respectively. The ClpP surface is colored according to the electrostatic surface potential and ranges from red (potential of −4kT) to blue (potential of +4kT) calculated using DelPhi (Rocchia et al., 2002). Also shown on the right panels are stick models of ACP1 docked into the H and C pockets of ClpP drawn as ribbons colored by chain. For ACP1, C, N, O, S, F, and H are colored in orange, blue, red, yellow, cyan, and white, respectively. All molecular graphics figures were prepared using the program PyMOL.

(C) Effect of mutations in the H and C pockets on ClpP activation by compounds measured using RD25. Data shown represent the average of three repeats and error bars give the standard deviations on the measurements (see also Figure S4B).

mutational analysis, involved in compound binding (Figure 6C). It is likely that the binding of compounds in the H pocket mimics the binding of ATPase chaperones and causes conformational changes in the ClpP axial pore, which normally occur upon binding of the Clp ATPase. The ADEP compounds, being much larger and bulkier, make more contacts in the ClpP binding pocket than the ACPs. The ACP compounds make fewer contacts, yet still induce ClpP activation. How these dissimilar compounds can cause the same effects warrants further investigation. Cocrystallization trials are currently under way to gain further understanding of the interaction of these compounds with ClpP.

In summary, our study identified new activators of ClpP that we term ACPs. These activators can be purchased relatively cheaply from regular vendors allowing any group to study this phenomenon without the need to rely on difficult purification procedures of natural products or complicated chemical synthesis methods. We expect that activators of self-compartmentalizing proteases will be important players in future drug development efforts.

SIGNIFICANCE

With the rise of antibiotic-resistant bacteria, there is an urgent need for the development of new compounds having novel mode of function. The ability to dysregulate ClpP serine protease activity represents a novel approach for the development of new antibacterials. ClpP activity is tightly regulated by bound ATPase chaperones. These ATPases typically form hexameric rings that bind on one or both ends of the ClpP double-ring cylinder. The ATPases select target substrates, which are then unfolded and threaded through the ATPase ring and into the ClpP cylinder for degradation. Threading into the ClpP proteolytic chamber occurs through narrow axial pores that do not allow structured proteins to pass, hence, the requirement for protein unfolding. Acyldepsipeptides, ADEPs, were recently found to bind ClpP and open the axial pores of the protease allowing ClpP to degrade folded proteins independent of its chaperone resulting in unregulated degradation of protein substrates. ADEPs were found to have antibacterial activity and were originally purified from *Streptomyces*. However, the chemical synthesis of these compounds is quite challenging. In order to identify novel compounds that activate ClpP, we used a high-throughput screening approach with a fluorescence-based readout. The assay employed fluorescein isothiocyanate-labeled casein as the proteolytic target of the *Escherichia coli* ClpP protease. Five structurally diverse compounds were identified to activate ClpP that we named Activators of Self-Compartmentalizing Proteases 1 to 5 (ACP1–5). Their chemical structures differ significantly from the structures of the ADEPs. The chemical optimization of ACP1 resulted in analogs having improved bioactivity and bactericidal effects. The compounds were found to stabilize the ClpP double-ring structure and to bind in pockets on the ClpP apical surface. Hence, our study provides the basis for the development of novel antibiotics based on the activation and dysregulation of ClpP activity using different structural scaffolds.

EXPERIMENTAL PROCEDURES

Protein Expression and Purification

All proteins were expressed from IPTG inducible promoters. ClpP constructs were expressed in BL21(DE3)1146D strain, which lacks the gene for chromosomal *E. coli* ClpP. All other constructs were expressed in BL21(DE3)Gold (Stratagene). Untagged WT and mutant *E. coli* ClpP, ClpX, and GFP-SsrA were expressed and purified as previously described (Wojtyra et al., 2003). ClpA was expressed and purified as described in Lo et al. (2001). All His-tagged proteins were purified on Ni-NTA agarose resin (QIAGEN) according to the manufacturer's protocols. If possible, the tag was removed using the tobacco etch virus (TEV) protease. Protein concentrations were determined by absorbance at 280 nm with extinction coefficients calculated using ProtParam (http://ca.expasy.org/tools/protparam.html).

Tah1 (Zhao et al., 2008) and λO (Wojtyra et al., 2003) were purified as previously described. pHF010 plasmid encoding H_6-λN was a kind gift from Dr. Irene Lee (Case Western Reserve University) and the protein was purified according to published protocols (Patterson-Ward et al., 2009). CFTR R-domain and α-synuclein were gifts from Dr. Julie Forman-Kay (University of Toronto). The Neisseria α-M protein was from Mr. Shekeb Khan from EFP's group. Reduced carboxymethylated α-lactalbumin was a gift from Dr. John Glover (University of Toronto). Creatine kinase, α-casein, casein fluorescein isothiocyanate (casein-FITC, type II, 20–50 μg FITC/mg, catalog number C3777), and N-Succinyl-Leu-Tyr-7-amido-4-methylcoumarin (Suc-LY-AMC) were purchased from Sigma-Aldrich.

Chemical Libraries and High-Throughput Screening

The libraries employed for the screening campaigns were composed of experimental bioactives, pharmacologically active chemicals and natural products, off-patent marketed drugs, and small molecules with drug-like properties. Samples were obtained from the following, commercially available collections: LOPAC 1280 (Sigma, 1280 samples), Prestwick Chemical library (Prestwick Chemical, France, 1120 samples), SPECTRUM collection (MicroSource, 2000 samples), Maybridge Screening collection (Maybridge-Thermo Fisher Scientific, UK, 50,000 samples), and Chembridge DIVERSet (ChemBridge Corp, 10,000 samples). In all instances, samples stored in 384-well plates as 1 or 5 mM solutions in 100% DMSO were transferred to assay plates in a fixed volume of 200 nl by a pin-tool (V&P Scientific). Screens were conducted using a fully automated procedure run on a DIM4 flipmover platform (Thermo Electron Corp) equipped with a Biomek FX liquid handler (Beckman, USA) and a PHERAStar detection system (BMG Labtech, Germany). The reaction for the screening assay contained 20 μM compound, 3.6 μM ClpP, and 4.5 μM casein-FITC in buffer A (25 mM Tris HCl [pH 7.5], and 100 mM KCl) at 37°C.

Compounds that were identified and confirmed to be hits were obtained from the following companies: ACP1, ACP2, and ACP3 are from Maybridge (Maybridge, Thermo-Fisher Scientific, catalog number BTB09142, JFD02943, and KM11066, respectively); ACP4 and ACP5 are from Chembridge (ChemBridge Corporation, catalog number 5107477 and 5107473, respectively).

Activity Assays

To measure the RD index, each reaction consisted of 3.6 μM ClpP and a specified amount of compound in buffer A. The reactions were preincubated for 10 min at 37°C before 4.5 μM casein-FITC and 15.5 μM unlabeled casein were added. ClpAP-dependent degradation of the same casein-FITC substrate was used as a control. Each ClpAP reaction contained 3.6 μM ClpP, 3 μM ClpA, and 0.3 mM ATP in buffer B (25 mM HEPES [pH 7.5], 20 mM $MgCl_2$, 30 mM KCl, 0.03% Tween 20, and 10% glycerol), and an ATP-regenerating system (13 units/ml of creatine kinase and 16 mM creatine phosphate). The reaction was started by adding casein-FITC. Reactions were incubated at 37°C and the fluorescence (485 nm excitation, 535 nm emission) was monitored every 15 min for 6 hr on a PHERAStar detection system. Casein-FITC degradation by compound-activated ClpP after 6 hr at 37°C was compared with the ClpAP-dependent casein-FITC degradation after 6 hr at 37°C, using Equation 1.

The effects of the compounds on the degradation of GFP-ssrA by ClpXP were also analyzed on SDS-PAGE gels. Each reaction contained 1.2 μM ClpP, 3.9 μM GFP-ssrA, 3 mM ATP, and 100 μM compound in buffer C (25 mM HEPES [pH 7.5], 5 mM $MgCl_2$, 5 mM KCl, 0.03% Tween 20, and

10% glycerol), and an ATP-regenerating system. The reaction mixtures were preincubated for 3 min at 37°C before 1 μM ClpX was added. Samples were taken at various time points, stopped by boiling in 2% SDS, and resolved on 12% SDS-PAGE gels.

Peptidase activity of ClpP was measured by the ability of ClpP to cleave the dipeptide Suc-LY-AMC. Each reaction contained 1 μM ClpP in buffer D (50 mM Tris HCl [pH 8], 200 mM KCl, and 1 mM DTT). ClpP was incubated for 3 min at 37°C before Suc-LY-AMC was added to a final concentration 0.5 mM. Fluorescence (350 nm excitation, 460 nm emission) of the released AMC was detected on the PHERAStar system.

For the Hill plot analysis of Figure 4B, each reaction consisted of 3.6 μM ClpP and specified amount of compound in buffer A. The reactions were pre-incubated for 10 min at 37°C before 4.5 μM casein-FITC was added. Reactions were incubated at 37°C and the fluorescence (485 nm excitation, 535 nm emission) was monitored every 3 s for 5 min on an EnSpire Multilabel Plate Reader (PerkinElmer).

N. meningitidis H44/76 *clpP* Insertional Mutagenesis

To construct the *N. meningitidis* H44/76 *clpP* insertional mutant vector, designated Nme-clpP-ery, primers f2 and r2 shown in Figure S2A were used to amplify a fragment of the genome that contained the *clpP* gene and the resulting PCR fragment was cloned into the pTrc99A vector. Using the f3 and r1 primers (Figure S2A), an erythromycin cassette with EagI ends was amplified from the pFLOB4300 vector (Litt et al., 2000) and the resulting PCR fragment was cloned into the EagI restriction site located at the 5′ end of the *clpP* gene within the Nme-clpP vector. The *N. meningitidis* H44/76 *clpP* insertional mutant was generated by transforming WT *N. meningitidis* H44/76 with the Nme-clpP-ery vector using an electroporation protocol adapted from (Dillard, 2006). PCR verification of the mutant strain is shown in Figure S2A.

Determination of Minimum Bactericidal Concentrations

Bacterial strains used included both gram-negative and gram-positive bacteria: *Escherichia coli* DH5α, *Salmonella typhimurium* SL1344, *Pseudomonas aeruginosa* PAO1, *Haemophilus influenzae* H2192, *Neisseria gonorrhoeae* N.279, *Neisseria meningitidis* H44/76, *Neisseria meningitidis* MC58, *Staphylococcus aureus* ATCC 29213, *Streptococcus pneumoniae* ATCC 49619, and *Listeria monocytogenes* EGD. Due to the low water solubility of the ADEP and ACP compounds, minimum bactericidal concentrations (MBC) values were determined by plating compound-treated bacteria on agar plates without compound. All compounds were diluted in Brain Heart Infusion (BHI) medium with 1% Isovitale X (Becton Dickinson). All bacteria were also inoculated into BHI. A 2-fold dilution series of each compound was created in 96-well plates, with and without 120 μg/ml of the membrane permeabilizing agent polymyxin B nonapeptide, PMBN (Sigma-Aldrich) (Ofek et al., 1994; Tsubery et al., 2002). All bacterial suspensions were pelleted, resuspended in BHI, and added to the compound containing media. *H. influenzae*, *N. gonorrhoeae*, and *N. meningitidis* were incubated 18–20 hr, while the remaining strains were incubated 12 to 16 hr. *H. influenzae*, *N. gonorrhoeae*, *N. meningitidis*, and *S. pneumoniae* were incubated in the presence of 5% CO_2. 2 μl of culture from the incubations were then plated onto compound-free agar plates (*H. influenzae*, *N. gonorrhoeae*, *N. meningitidis* for 18–20 hr; remaining strains for 12–16 hr) to determine the bactericidal activity. *H. influenzae* was grown on chocolate agar; *N. gonorrhoeae* on GC agar base; *N. meningitidis*, *S. aureus*, and *L. monocytogenes* on BHI agar; *S. pneumoniae* on 5% sheep blood agar; and *E. coli*, *S. typhimurium*, and *P. aeruginosa* on LB agar. The lowest concentration of compound at which no bacterial growth was seen was designated as the minimum bactericidal concentration.

Antimycobacterial activities of the ClpP activating compounds were investigated using the 96-well plate broth microdilution method modified from Wallace et al. (1986), followed by plating for viable bacteria. Compounds were dissolved in 100% DMSO. *M. smegmatis* mc^2155 cultures were grown to an OD_{600} of 1.0–1.3 in Middlebrook 7H9 broth (Difco, BD Biosciences) supplemented with 2% oleic acid, albumin, dextrose, and catalase (OADC enrichment, BD Biosciences) as well as 0.2% glycerol and 0.5% Tween 80 to avoid clumping of bacteria. Cultures were then diluted 10-fold and 5 μl were used to inoculate 100 μl of a 2-fold dilution series of compounds in the range of 1 μg/ml to 256 μg/ml in 7H9 broth supplemented with OADC and 0.2% glycerol in the presence or absence of 12.5 μg/ml polymyxin B. Polymyxin B is known to enhance mycobacterial permeability to hydrophobic compounds (Korycka-Machala et al., 2001). The solvent control, DMSO at 2% or less, showed no inhibitory effects on *M. smegmatis* growth. Plates were incubated in a CO_2 incubator for 8 days. Following incubation, dilutions of sample aliquots were spread on Middlebrook 7H11 plates (Difco, BD Biosciences) supplemented with 2% OADC and 0.5% glycerol for determination of bacterial viability.

Monitoring of *E. coli* Growth in the Presence of ACP Compounds

The *E. coli* strains used for growth curves shown in Figure S2D, MC4100 and MC4100 Δ*clpP*::*cat*, were grown overnight in LB and then diluted into fresh LB to OD_{600} of 0.02. One hundred microliters of the diluted cell culture was added to 100 μl of LB containing ACP1b and CCCP (carbonyl cyanide 3-chlorophenylhydrazone) (Sigma-Aldrich). Final concentrations were 128 μg/ml ACP1b and/or 20 μM CCCP. The solvent control cultures contained 20 μM CCCP and 2.2% DMSO in place of ACP1b. Growth was monitored overnight at 30°C in a Bioscreen-C incubator system (Growth Curves, USA).

Other Procedures

Additional methods are given in the Supplemental Experimental Procedures, namely, subcloning and mutagenesis, surface plasmon resonance measurements, isothermal titration calorimetry measurements, analytical ultracentrifugation measurements, thermal denaturation of ClpP, isolation of ADEP1A and ADEP1B from *Streptomyces hawaiiensis* NRRL 15010, docking procedure, and chemical synthesis of ACP1 and analogs.

SUPPLEMENTAL INFORMATION

Supplemental Information includes four figures, one table, and Supplemental Experimental Procedures and can be found with this article online at doi:10.1016/j.chembiol.2011.07.023.

ACKNOWLEDGMENTS

This work was supported by the Canadian Institutes of Health Research Emerging Team Grants from the Institute of Infection and Immunity (XNE-86945) to A.D., E.F.P., J.L., S.G.-O., R.A.B., and W.A.H. M.E.B. is the recipient of a fellowship from the Canadian Institutes of Health Research (CIHR) Strategic Training Program in Protein Folding and Interaction Dynamics: Principles and Diseases. S.J.W. is Canada Research Chair Tier 1, funded by the Canada Institute of Health Research.

Received: February 16, 2011
Revised: June 28, 2011
Accepted: July 13, 2011
Published: September 22, 2011

REFERENCES

Bewley, M.C., Graziano, V., Griffin, K., and Flanagan, J.M. (2006). The asymmetry in the mature amino-terminus of ClpP facilitates a local symmetry match in ClpAP and ClpXP complexes. J. Struct. Biol. *153*, 113–128.

Bewley, M.C., Graziano, V., Griffin, K., and Flanagan, J.M. (2009). Turned on for degradation: ATPase-independent degradation by ClpP. J. Struct. Biol. *165*, 118–125.

Brideau, C., Gunter, B., Pikounis, B., and Liaw, A. (2003). Improved statistical methods for hit selection in high-throughput screening. J. Biomol. Screen. *8*, 634–647.

Brötz-Oesterhelt, H., Beyer, D., Kroll, H.-P., Endermann, R., Ladel, C., Schroeder, W., Hinzen, B., Raddatz, S., Paulsen, H., Henninger, K., et al. (2005). Dysregulation of bacterial proteolytic machinery by a new class of antibiotics. Nat. Med. *11*, 1082–1087.

Creamer, L.K., Richardson, T., and Parry, D.A.D. (1981). Secondary structure of bovine alpha s1- and beta-casein in solution. Arch. Biochem. Biophys. *211*, 689–696.

Dillard, J.P. (2006). Genetic manipulation of Neisseria gonorrhoeae. Curr. Protoc. Microbiol. *Chapter 4*, Unit 4A 2.

Gottesman, S., Maurizi, M.R., and Wickner, S. (1997). Regulatory subunits of energy-dependent proteases. Cell *91*, 435–438.

Hinzen, B., Raddatz, S., Paulsen, H., Lampe, T., Schumacher, A., Häbich, D., Hellwig, V., Benet-Buchholz, J., Endermann, R., Labischinski, H., and Brötz-Oesterhelt, H. (2006). Medicinal chemistry optimization of acyldepsipeptides of the enopeptin class antibiotics. ChemMedChem *1*, 689–693.

Jennings, L.D., Lun, D.S., Médard, M., and Licht, S. (2008). ClpP hydrolyzes a protein substrate processively in the absence of the ClpA ATPase: mechanistic studies of ATP-independent proteolysis. Biochemistry *47*, 11536–11546.

Katayama, Y., Gottesman, S., Pumphrey, J., Rudikoff, S., Clark, W.P., and Maurizi, M.R. (1988). The two-component, ATP-dependent Clp protease of Escherichia coli. Purification, cloning, and mutational analysis of the ATP-binding component. J. Biol. Chem. *263*, 15226–15236.

Keller, T.H., Pichota, A., and Yin, Z. (2006). A practical view of "druggability". Curr. Opin. Chem. Biol. *10*, 357–361.

Kirstein, J., Hoffmann, A., Lilie, H., Schmidt, R., Rübsamen-Waigmann, H., Brötz-Oesterhelt, H., Mogk, A., and Turgay, A. (2009). The antibiotic ADEP reprogrammes ClpP, switching it from a regulated to an uncontrolled protease. EMBO Mol. Med. *1*, 37–49.

Korycka-Machala, M., Ziółkowski, A., Rumijowska-Galewicz, A., Lisowska, K., and Sedlaczek, L. (2001). Polycations increase the permeability of Mycobacterium vaccae cell envelopes to hydrophobic compounds. Microbiology *147*, 2769–2781.

Lang, P.T., Brozell, S.R., Mukherjee, S., Pettersen, E.F., Meng, E.C., Thomas, V., Rizzo, R.C., Case, D.A., James, T.L., and Kuntz, I.D. (2009). DOCK 6: combining techniques to model RNA-small molecule complexes. RNA *15*, 1219–1230.

Lee, B.G., Park, E.Y., Lee, K.E., Jeon, H., Sung, K.H., Paulsen, H., Rübsamen-Schaeff, H., Brötz-Oesterhelt, H., and Song, H.K. (2010). Structures of ClpP in complex with acyldepsipeptide antibiotics reveal its activation mechanism. Nat. Struct. Mol. Biol. *17*, 471–478.

Li, D.H., Chung, Y.S., Gloyd, M., Joseph, E., Ghirlando, R., Wright, G.D., Cheng, Y.Q., Maurizi, M.R., Guarné, A., and Ortega, J. (2010). Acyldepsipeptide antibiotics induce the formation of a structured axial channel in ClpP: A model for the ClpX/ClpA-bound state of ClpP. Chem. Biol. *17*, 959–969.

Lipinski, C.A., Lombardo, F., Dominy, B.W., and Feeney, P.J. (2001). Experimental and computational approaches to estimate solubility and permeability in drug discovery and development settings. Adv. Drug Deliv. Rev. *46*, 3–26.

Litt, D.J., Palmer, H.M., and Borriello, S.P. (2000). Neisseria meningitidis expressing transferrin binding proteins of Actinobacillus pleuropneumoniae can utilize porcine transferrin for growth. Infect. Immun. *68*, 550–557.

Lo, J.H., Baker, T.A., and Sauer, R.T. (2001). Characterization of the N-terminal repeat domain of *Escherichia coli* ClpA-A class I Clp/HSP100 ATPase. Protein Sci. *10*, 551–559.

Maurizi, M.R., and Xia, D. (2004). Protein binding and disruption by Clp/Hsp100 chaperones. Structure *12*, 175–183.

Michel, K.H., and Kastner, R.E. (1985). A54556 antibiotics and process for production thereof. (US Patent 4492650).

Mogridge, J., Legault, P., Li, J., Van Oene, M.D., Kay, L.E., and Greenblatt, J. (1998). Independent ligand-induced folding of the RNA-binding domain and two functionally distinct antitermination regions in the phage lambda N protein. Mol. Cell *1*, 265–275.

Ofek, I., Cohen, S., Rahmani, R., Kabha, K., Tamarkin, D., Herzig, Y., and Rubinstein, E. (1994). Antibacterial synergism of polymyxin B nonapeptide and hydrophobic antibiotics in experimental gram-negative infections in mice. Antimicrob. Agents Chemother. *38*, 374–377.

Ostedgaard, L.S., Baldursson, O., and Welsh, M.J. (2001). Regulation of the cystic fibrosis transmembrane conductance regulator Cl- channel by its R domain. J. Biol. Chem. *276*, 7689–7692.

Patterson-Ward, J., Tedesco, J., Hudak, J., Fishovitz, J., Becker, J., Frase, H., McNamara, K., and Lee, I. (2009). Utilization of synthetic peptides to evaluate the importance of substrate interaction at the proteolytic site of Escherichia coli Lon protease. Biochim. Biophys. Acta *1794*, 1355–1363.

Rocchia, W., Sridharan, S., Nicholls, A., Alexov, E., Chiabrera, A., and Honig, B. (2002). Rapid grid-based construction of the molecular surface and the use of induced surface charge to calculate reaction field energies: applications to the molecular systems and geometric objects. J. Comput. Chem. *23*, 128–137.

Tompa, P. (2009). Structural disorder in amyloid fibrils: its implication in dynamic interactions of proteins. FEBS J. *276*, 5406–5415.

Tsubery, H., Ofek, I., Cohen, S., Eisenstein, M., and Fridkin, M. (2002). Modulation of the hydrophobic domain of polymyxin B nonapeptide: effect on outer-membrane permeabilization and lipopolysaccharide neutralization. Mol. Pharmacol. *62*, 1036–1042.

Wallace, R.J., Jr., Nash, D.R., Steele, L.C., and Steingrube, V. (1986). Susceptibility testing of slowly growing mycobacteria by a microdilution MIC method with 7H9 broth. J. Clin. Microbiol. *24*, 976–981.

Wojtyra, U.A., Thibault, G., Tuite, A., and Houry, W.A. (2003). The N-terminal zinc binding domain of ClpX is a dimerization domain that modulates the chaperone function. J. Biol. Chem. *278*, 48981–48990.

Zhang, J.-H., Chung, T.D.Y., and Oldenburg, K.R. (1999). A Simple Statistical Parameter for Use in Evaluation and Validation of High Throughput Screening Assays. J. Biomol. Screen. *4*, 67–73.

Zhao, R., Davey, M., Hsu, Y.C., Kaplanek, P., Tong, A., Parsons, A.B., Krogan, N., Cagney, G., Mai, D., Greenblatt, J., et al. (2005). Navigating the chaperone network: an integrative map of physical and genetic interactions mediated by the hsp90 chaperone. Cell *120*, 715–727.

Zhao, R., Kakihara, Y., Gribun, A., Huen, J., Yang, G., Khanna, M., Costanzo, M., Brost, R.L., Boone, C., Hughes, T.R., et al. (2008). Molecular chaperone Hsp90 stabilizes Pih1/Nop17 to maintain R2TP complex activity that regulates snoRNA accumulation. J. Cell Biol. *180*, 563–578.

Chemistry & Biology *18*

Supplemental Information

Activators of Cylindrical Proteases as Antimicrobials: Identification and Development of Novel Small Molecule Activators of ClpP Protease

Elisa Leung, Alessandro Datti, Michele Cossette, Jordan Goodreid, Shannon E. McCaw, Michelle Mah, Alina Nakhamchik, Koji Ogata, Majida El Bakkouri, Yi-Qiang Cheng, Shoshana J. Wodak, Bryan T. Eger, Emil F. Pai, Jun Liu, Scott Gray-Owen, Robert A. Batey, and Walid A. Houry

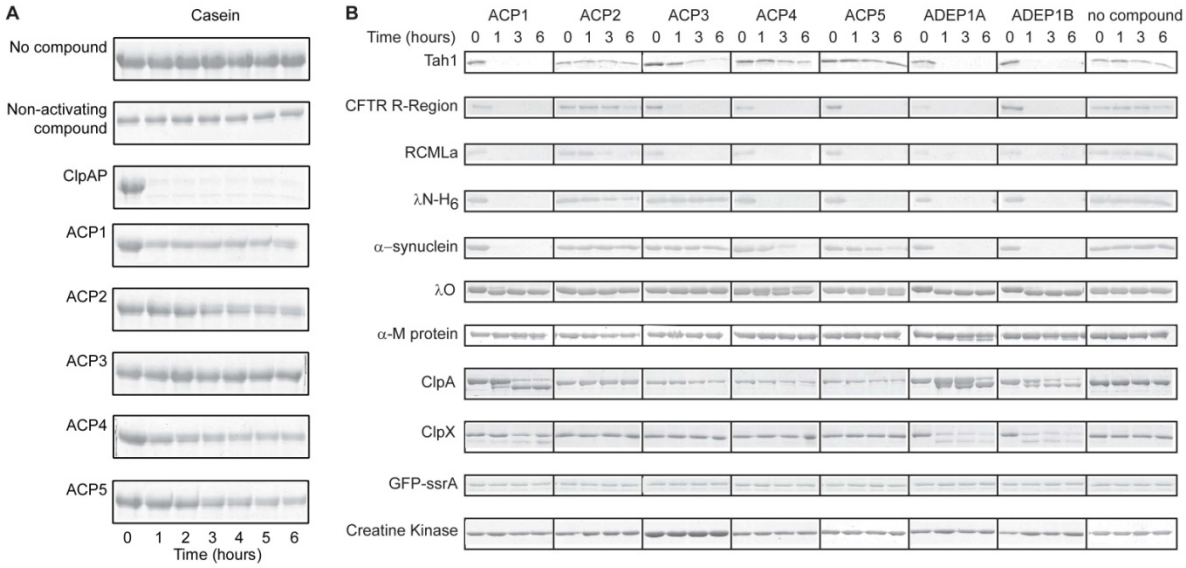

C

Substrate	*MW* (kDa)	Activator						
		ADEP1A	ADEP1B	ACP1	ACP2	ACP3	ACP4	ACP5
Bovine α-casein	25	++	++	++	++	++	++	++
Yeast Tah1	13	++	++	++	++	++	++	++
Human CFTR R-Domain	33	++	++	++	++	++	++	++
Bovine reduced carboymethylated α-lactalbumin	14	++	++	++	++	++	++	++
Bacteriophage λN-H_6	15	++	++	++	++	-	++	++
Human α-synuclein	18	++	++	++	-	-	++	++
Bacteriophage λO	33	+	+	+	-	-	+	+
Neisseria α-M protein	44	+	+	+	-	-	-	-
E. coli ClpA	84	+	+	+	-	-	-	-
E. coli ClpX	50	+	+	+	-	-	-	-
Jellyfish green fluorescent protein-ssrA	27	-	-	-	-	-	-	-
Rabbit creatine kinase	43	-	-	-	-	-	-	-

FIGURE S2

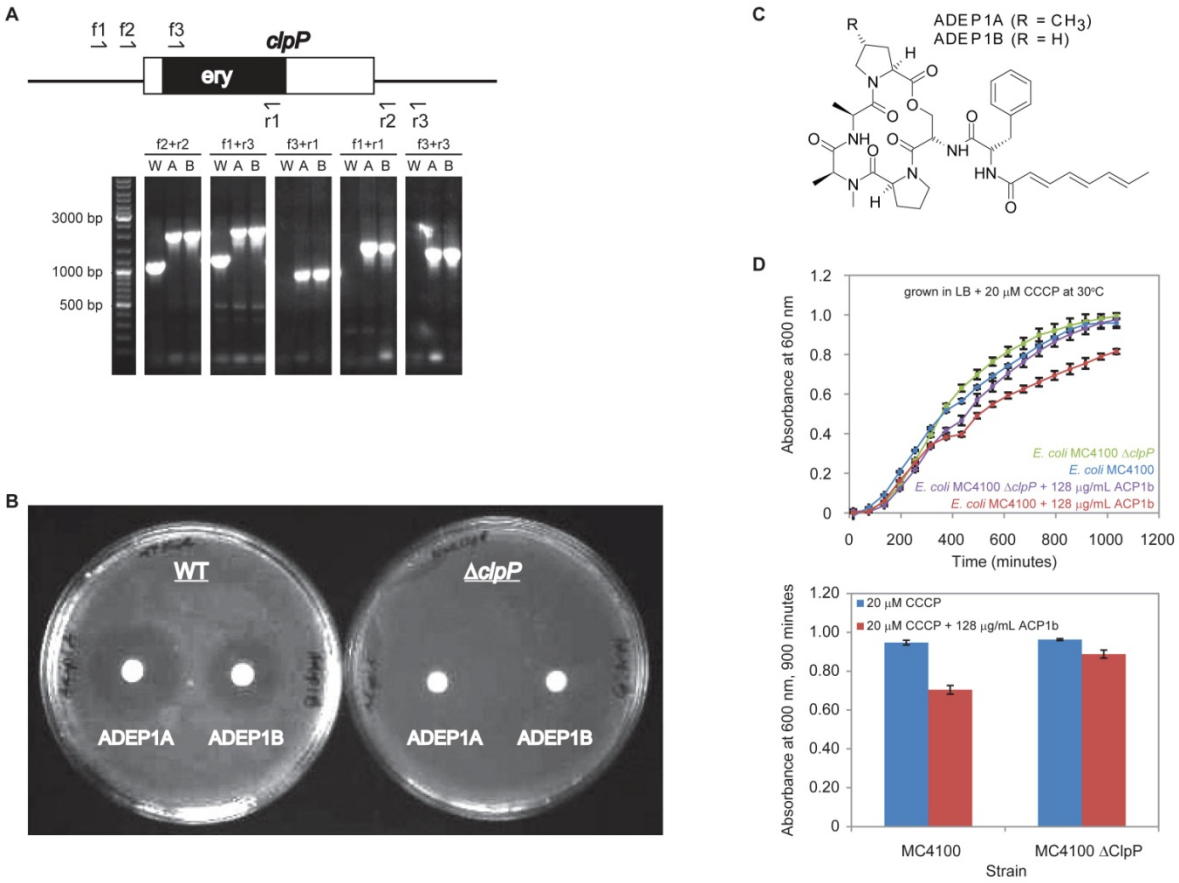
A
f1 f2 f3
clpP
ery
r1 r2 r3
f2+r2 f1+r3 f3+r1 f1+r1 f3+r3
W A B W A B W A B W A B W A B
3000 bp
1000 bp
500 bp
B
WT
ΔclpP
ADEP1A ADEP1B ADEP1A ADEP1B
C
ADEP1A (R = CH3)
ADEP1B (R = H)
D
grown in LB + 20 μM CCCP at 30°C
Absorbance at 600 nm
Time (minutes)
E. coli MC4100 ΔclpP
E. coli MC4100
E. coli MC4100 ΔclpP + 128 μg/mL ACP1b
E. coli MC4100 + 128 μg/mL ACP1b
Absorbance at 600 nm, 900 minutes
20 μM CCCP
20 μM CCCP + 128 μg/mL ACP1b
MC4100
MC4100 ΔClpP
Strain

FIGURE S3

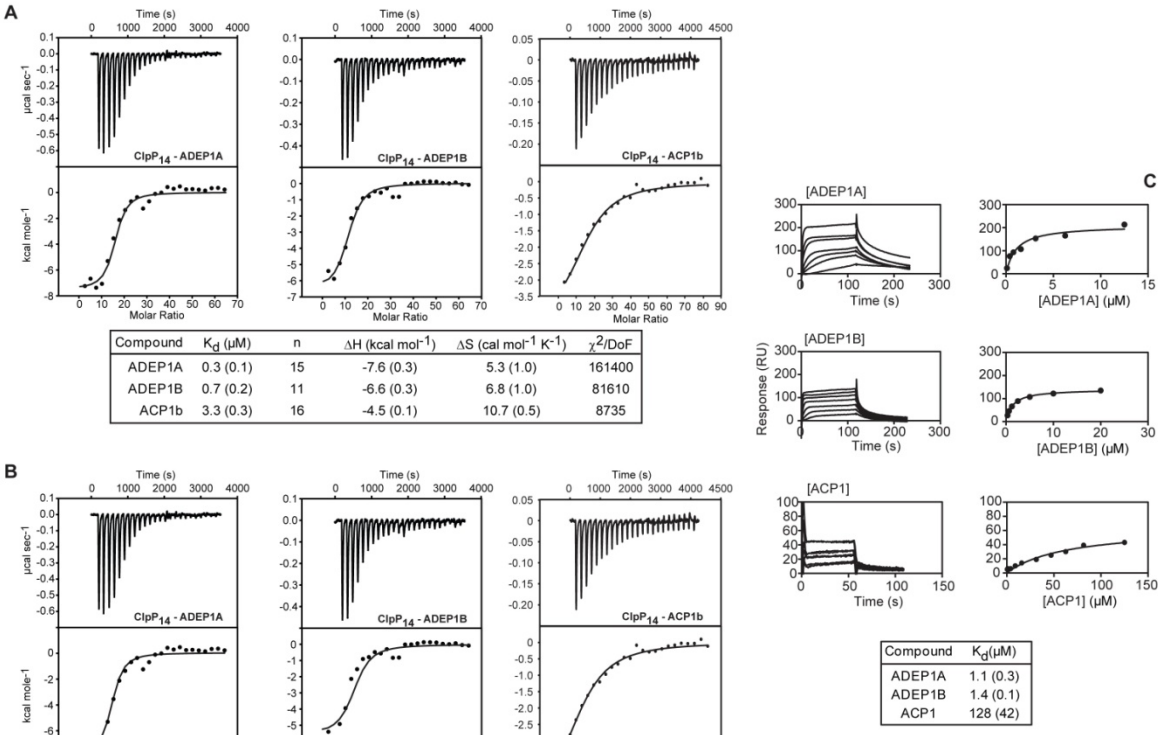

Compound	K_d (µM)	n	ΔH (kcal mol^{-1})	ΔS (cal mol^{-1} K^{-1})	χ^2/DoF
ADEP1A	0.3 (0.1)	15	-7.6 (0.3)	5.3 (1.0)	161400
ADEP1B	0.7 (0.2)	11	-6.6 (0.3)	6.8 (1.0)	81610
ACP1b	3.3 (0.3)	16	-4.5 (0.1)	10.7 (0.5)	8735

Compound	K_d (µM)	n	ΔH (kcal mol^{-1})	ΔS (cal mol^{-1} K^{-1})	χ^2/DoF
ADEP1A	0.4 (0.1)	14	-7.9 (0.3)	4.0 (1.1)	165100
ADEP1B	0.7 (0.3)	14	-5.6 (0.4)	9.9 (1.0)	206700
ACP1b	4.1 (0.4)	14	-5.2 (0.2)	7.8 (0.6)	10160

Compound	K_d(µM)
ADEP1A	1.1 (0.3)
ADEP1B	1.4 (0.1)
ACP1	128 (42)

FIGURE S4

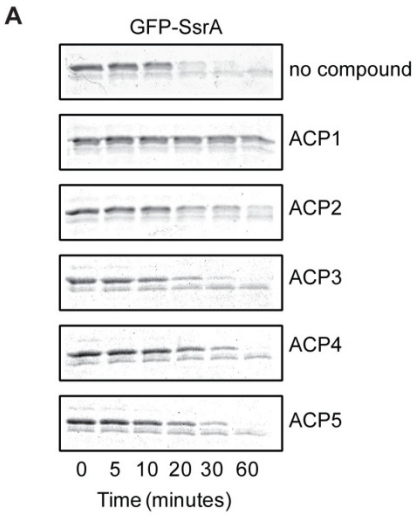

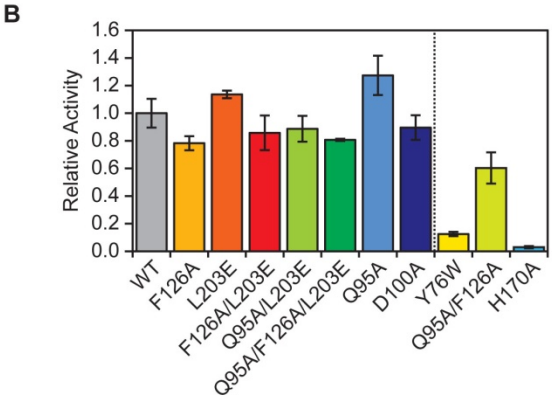

	H pocket mutants	H &C pocket mutants	C pocket mutants
WT	F126A	Q95A/L203E	Q95A
	L203E	Q95A/F126A/L203E	D100A
	F126A/L203E	Q95A/F126A	H170A
	Y76W		

Fig. S1. Confirmation of ClpP activation by the hits identified in the high-throughput screen (related to **Fig. 1**).
(**A**) The disappearance of unlabeled casein due to degradation by compound-activated ClpP was followed over time on SDS-PAGE gels, which were then stained with Coomassie Brilliant Blue.
(**B**) Shown is the degradation of the indicated substrates by compound-activated ClpP followed on SDS-PAGE gels for 6 hours.
(**C**) Summary of the ClpP degradation assays with alternative substrates. The double plus (+ +) denotes complete substrate degradation, the single plus (+) denotes partial degradation or clipping of the substrate, and the hyphen (-) denotes no visible degradation.

Fig. S2. Loss of *clpP* confers resistance to ADEP and ACP in *N. meningitidis* H44/76 and *E. coli* MC4100 (related to **Fig. 3**).
(**A**) PCR verification of *clpP* insertional mutagenesis *N. meningitidis* H44/76. Genomic DNA recovered from wild type (W) or erythromycin-resistant *N. meningitidis* H44/76 transformants (A and B, representing two replicate samples) were used as template for PCR with the indicated primer pairs. The schematic depicts relative location of oligonucleotide primer sequences on the genome of the *clpP* mutant bacteria.
(**B**) Fresh overnight cultures of *N. meningitidis* H44/76 were spread onto the surface of standard growth media, and filter discs impregnated with 256 μg/mL of ADEP1A or ADEP1B were laid on the surface. Zones of clearing on plates cultured with WT meningococci reflect inhibition of bacterial growth, whereas no inhibitory effect of either compound was apparent on plates cultured with the meningococcal *clpP* mutant.
(**C**) The chemical structures of ADEP1A and ADEP1B.
(**D**) Upper panel shows the growth curves for WT and Δ*clpP E. coli* MC4100 in the presence of 20 μM CCCP or 20 μM CCCP + 128 μg/mL ACP1B in LB at 30°C. The curves shown represent the average of 3 cultures. The lower panel shows OD_{600} at 900 minutes for the two strains.

Fig. S3. Binding of ClpP to ADEP1A, ADEP1B, and ACP1b (related to **Fig. 4**).
(**A**) ITC binding curves for ClpP-ADEP1A, ADEP1B, or ACP1b interaction. Results for the fit of the data to a one set of identical independent binding site model is given in the table. The number of binding sites, n, were fixed in the fit to the indicated whole number. Numbers in parentheses refer to standard deviations. χ^2/DoF refers to chi-squared divided by the degrees of freedom and indicates the quality of the fit (see also **Fig. 4A**).
(**B**) Same as **A**, but n was fixed to 14.
(**C**) SPR analysis for the binding of ClpP with the different activators. Graphs on the left represent the stacked sensorgrams from SPR experiments of compounds at various concentrations injected over a biosensor chip surface immobilized with ClpP. Graphs on the right depict the binding curves constructed with the steady state data fit to a one-site Langmuir binding model. The K_d and the respective standard deviations obtained by the fits are listed in the table at the bottom.

Fig. S4. The binding of ACPs to the H and C pockets on ClpP (related to **Fig. 6**).
(**A**) Inhibition of ClpXP-mediated GFP-ssrA degradation by ACPs. 100 μM of ACP1-5 inhibited or reduced GFP-SsrA degradation by ClpXP as monitored on SDS-PAGE gels.
(**B**) Effect of mutations in the H and C pockets on ClpP peptidase activity. Peptidase assays were carried out comparing the peptide hydrolysis activities of various *E. coli* ClpP mutants against

the Suc-LY-AMC peptide. Mutations were made in the H pocket, C pocket, or in combination. The color scheme is the same as that for **Fig. 6C**. Values were normalized to the wild type ClpP peptide hydrolysis rate. Mutants with peptidase activity less than 70% of WT are grouped on the right. Data shown represent the average of three repeats and the error bars represent the standard deviations.

Table S1. Docking data related to Figure 6B.

Lowest Dock6 score for ACP compounds

Name of Compound	Dock6 Score	
	H pocket	C pocket
ACP1	-43.36	-42.05
ACP2	-74.50	-71.10
ACP3	-37.91	-39.72
ACP4[a]	-40.00	-44.11
ACP5[b]	-38.78	-40.02

ACP4 chiral isomers

ID[c]	X_1	X_2	X_3
ACP4_SSS	S	S	S
ACP4_SSR	S	S	R
ACP4_SRS	S	R	S
ACP4_SRR	S	R	R
ACP4_RSS	R	S	S
ACP4_RSR	R	S	R
ACP4_RRS	R	R	S
ACP4_RRR	R	R	R

ACP5 chiral isomers

ID[d]	X_1	X_2	X_3
ACP5_SSS	S	S	S
ACP5_SSR	S	S	R
ACP5_SRS	S	R	S
ACP5_SRR	S	R	R
ACP5_RSS	R	S	S
ACP5_RSR	R	S	R
ACP5_RRS	R	R	S
ACP5_RRR	R	R	R

[a]ACP4_SSR and ACP4_RRS showed the lowest Dock6 score values on H and C pockets, respectively.

[b]ACP5_RRS and ACP5_SRR showed the lowest Dock6 score values on H and C pockets, respectively.

[c]ACP4 is ethyl ($1X_1$,$2X_2$,$4X_3$)-2-(2,2-dichloroethenyl)-4-hydroxy-4-(4-nitrophenyl)-6-oxocyclohexane-1-carboxylate in IUPAC nomenclature, where X_1, X_2, and X_3 can adopt either S or R chirality.

[d]ACP5 is ethyl ($1X_1$,$2X_2$,$4X_3$)-4-(4-bromophenyl)-2-(2,2-dichloroethenyl)-4-hydroxy-6-oxocyclohexane-1-carboxylate in IUPAC nomenclature, where X_1, X_2, and X_3 can adopt either S or R chirality.

SUPPLEMENTARY EXPERIMENTAL PROCEDURES

Subcloning and mutagenesis

The plasmids pET9a ClpP and pET9a ClpA(M169T) for overexpressing the respective *E. coli* proteins were generous gifts from Dr. John Flannagan (Brookhaven National Laboratory, NY, USA). The M169T mutation in ClpA removes an internal translation initiation site (Lo et al., 2001). ClpA(M169T) is referred to as ClpA throughout this paper.

The coding sequences for genes to overexpress *E. coli* ClpPΔ31 were amplified from the pET9a ClpP plasmid and inserted between the NdeI and BamHI sites of pET3a. Full length ClpP point mutants were constructed using mutagenic primers to the pET9a ClpP plasmid and the QuickChange system (Stratagene).

Surface Plasmon Resonance (SPR) measurements

SPR measurements were conducted on a BiacoreX instrument (GE Healthcare) at 25°C. ClpP was immobilized on CM5 chips (GE Healthcare) using the Biacore amine coupling kit (GE Healthcare) following the manufacturer's protocols. One flow cell was immobilized with ClpP, while the other was activated and deactivated without protein immobilization. The sensorgrams in the sham activated-deactivated control surface were subtracted from the corresponding sensorgrams in the ClpP immobilized flow cell to remove the effect of nonspecific binding to the chip surface and the bulk effect from the buffer. Binding experiments were performed at 20 μL/minute in running buffer E (20 mM TrisHCl, pH 7.5, 100 mM KCl, 3 mM EDTA, 0.005% P20 surfactant, and 5% DMSO). An association phase of a 60 or 120 seconds injection of compound was followed by a dissociation phase of 60 or 120 seconds of running buffer flow before the chip and sample loop were washed at high flow rate. The surface was regenerated between injections with a one minute pulse of 10% DMSO in running buffer E. The steady state responses were plotted versus the corresponding analyte concentrations and fit to one-site

Langmuir binding models using BiaEvaluation 4.1 software (GE Healthcare).

Isothermal Titration Calorimetry (ITC)

Experiments were performed at 37°C using a Microcal VP-ITC isothermal titration calorimeter (GE Healthcare). The 1.4 mL sample cell was filled with 10 μM ClpP in buffer F (25 mM TrisHCl, pH 7.5, 100 mM KCl, and 1% DMSO) and stirred constantly at 270 rpm. The syringe was filled with 250 μM compound and titrated into the sample cell in one 1 μL injection, followed by 10 μL injections at 170 seconds intervals. After the background heats of dilution from the titration of compound into buffer were subtracted from the experimental data, the net binding data were fit by least squares regression to a model corresponding to one set of identical independent binding sites using Origin 7.0 software (OriginLab, MA, USA).

Analytical ultracentrifugation

Analytical ultracentrifugation experiments were carried out at the Ultracentrifugation Service Facility, Department of Biochemistry, University of Toronto. 1 mg/mL ClpP was exchanged into buffer B containing 100 μM compound by dialysis. For sedimentation velocity experiments, samples were spun at 45,500 g at 4°C in a Beckman Optima Model XL-A analytical ultracentrifuge equipped with an An-60 Ti rotor. The density (ρ=1.00545) and viscosity of buffer (η=1.57x10^{-2}) and the partial specific volumes of ClpPΔ31 (vbar=0.7319) were calculated using SedNterp (Laue et al., 1992). The sedimentation data were fit to a continuous distribution model c(S) using SEDFIT (Schuck, 2000). The observed sedimentation coefficients obtained from the fits were corrected to the density and viscosity of water at 20°C to obtain $s_{20,w}$. The molar mass reported for each sedimentation coefficient peak in the size distribution was estimated by the SEDFIT software using the frictional ratio from the fit and the partial specific volume for ClpPΔ31.

For sedimentation equilibrium experiments, samples were spun at 7000, 9000, and 11000 rpm at 4°C in a Beckman Optima XL-A analytical ultracentrifuge equipped with an An-60 Ti rotor. Absorbance was monitored at 280 nm. Data analysis was performed using the Origin MicroCal XL-A/CL-I Data Analysis Software Package version 4.0.

Thermal denaturation of ClpP

Thermal melting of ClpP in the presence and absence of activating compounds was performed on a Jasco J-810 circular dichroism spectrophotometer. Proteins and compounds were diluted into buffer A to a concentration of 25 μM ClpP and 80 μM compound. DMSO (from the compound stock solution) accounted for no more than 0.16% v/v of the solution.

Isolation of ADEP1A and ADEP1B from *Streptomyces hawaiiensis* NRRL 15010

Bacterial strain *Streptomyces hawaiiensis* NRRL 15010 was obtained from the US Agricultural Research Service Culture Collection (NRRL). Amberlite XAD16 resin and Diaion HP-20 resin were purchased from Sigma-Aldrich (St. Louis, MO). All other chemicals and solvents were from Fisher Scientific (Pittsburgh, PA) and its associated providers. A54556 factor A and B, referred to as ADEP1A and ADEP1B, respectively, were purified to at least 95% homogeneity from the fermentation culture of *S. hawaiiensis*, according to Michel and Kastner (Michel and Kastner, 1985) with slight modification. Specifically, 20 liters of fermentation medium (0.4% D-glucose, 0.4% yeast extract, 1.0% malt extract, 0.1% $CaCO_3$, 1.0% Diaion HP-20 resin, and 1.0% Amberlite XAD16 resin in tap water, pH 7.2) was inoculated with 200 mL of overnight seed culture, divided into 40 flasks (500 ml per 2-L flask), and cultivated for 4 days at 30°C on a rotary shaker (200 rpm). Culture filtrate and residue (resin, mycelia and cell debris) were separated by filtration. The filtrate was extracted with equal volume of ethyl acetate for 3 times and the residue was extracted with 2-fold volume of ethyl acetate for 5 times. The ethyl acetate

extracts were combined and evaporated under reduced pressure to an oily dense residue. The residue was dissolved in methanol and subjected sequentially to normal phase silica gel gravity chromatography (eluting with chloroform/methanol), C-18 reverse phase silica gel (ODS) gravity chromatography (eluting with methanol/water), and C-18 reverse phase silica gel preparative high performance liquid chromatography (HPLC; eluting with methanol/water). Fractions containing the target compounds were monitored by electro-spray ionization mass spectrometry (ESI-MS). The final compound preparations were verified by mass spectrometry and nuclear magnetic resonance analyses, and stored as amorphous dry powder.

Docking procedure

Initial structures of ACP1, ACP2 and ACP3 were obtained from the PubChem database (Wang et al., 2009). Those of ACP4 and ACP5 were generated by the Marvin Beans software package (Marvin Beans 4.1.5, ChemAxon Ltd., Budapest, 2007). ACP4 and ACP5 have 8 chiral isomers each arising from three chiral carbons in the oxocyclohexane moiety (**Table S1**). The 19 resulting ACP structures (one each for ACP1, ACP2, and ACP3, and 8 chiral structures for each of ACP4 and ACP5) were minimized using the Steepest Decent algorithm and the MMFF94 force field implemented in the OpenBabel software package (Guha et al., 2006). The structure of ClpP used in the docking procedure was that of *E. coli* ClpP (PDB code 1yg6) (Bewley et al., 2006). A dimer of the neighboring chains A and G in the PDB entry were extracted from one heptameric ring of ClpP and used for docking procedures.

The DOCK6.3 package (Lang et al., 2009) was used to dock the flexible conformations of the five compounds into the structure of ClpP, which was kept rigid. For each compound the 'anchor and grow' method was used with default options. The docking poses for each compound structure were ranked using the standard DOCK scoring function (**Table S1**), which is based on the AMBER molecular mechanics force field. This scoring function includes contributions from

van der Waals and Coulomb interactions. The latter were screened using a distance dependent dielectric constant (ε=4r, where r is the interatomic distance), but no cut-off was used for the non-bonded interactions. The 10 highest ranking poses and conformations were retained for further analysis.

Prior to executing the docking calculations, the SPHGEN algorithm (Kuntz et al., 1982) was used to identify ligand binding pockets on the surface of the ClpP dimer facing ClpX. Two pockets were predicted: one largely hydrophobic pocket corresponding to the ClpX IGF loop binding cleft was designated as the H pocket. The second pocket, located nearby, was designated as the C pocket. Docking calculations were performed separately for the H and C pockets, with boxes for the grid-based scoring function (grid spacing of 0.3Å) generated from the output of SPHGEN for each pocket.

Chemical synthesis of ACP1 and analogs

ACP1 and its analogs were typically prepared using conventional amide bond-coupling conditions between the acid and amine components. PyBOP ((benzotriazol-1-yl-oxy)tripyrrolidinophosphonium hexafluorophosphate) was established as the most effective reagent for amide couplings. The precursor acid and amines were synthesized using standard methods.

Representative Procedure: A solution of 2-methyl-2-((5-(trifluoromethyl)pyridin-2-yl)sulfonyl)propanoic acid (20 mg, 0.067 mmol) in anhydrous DMF (2.0 mL) was treated with a solution of PyBOP (38 mg, 0.074 mmol) in anhydrous DMF (0.5 mL) followed by diisopropylethylamine (35 μL, 0.20 mmol). A solution of the amine (0.067 mmol) in anhydrous DMF (0.5 mL) was then added dropwise. The resulting yellow solution was stirred at room temperature for 1 hr. The DMF was removed *in vacuo* and the crude product was absorbed onto silica gel. The product was purified by column chromatography (silica gel, EtOAc/hexanes).

Representative Characterization Data: 2-Methyl-*N*-(3-phenylpropyl)-2-((5-(trifluoromethyl)pyridin-2-yl)sulfonyl)propanamide (ACP1a) obtained in 88 % yield as a white solid from ethyl acetate and hexanes. R_f = 0.26 (25 % v/v ethyl acetate in hexanes), mp 83–86°C; ^{1}H NMR (300 MHz, $CDCl_3$) δ 8.90 (1H, s), 8.20–8.16 (2H, m), 7.35–7.25 (2H, m), 7.25–7.15 (3H, m), 7.06–6.90 (1H, br m), 3.38–3.28 (2H, m), 2.71 (2H, t, *J* = 7.5 Hz), 1.92 (2H, tt, J = 7.5 Hz, 7.5 Hz), 1.62 (6H, s); ^{13}C NMR (75 MHz, $CDCl_3$) δ 167.4, 158.3 (q, *J* = 1.4 Hz), 147.3 (q, *J* = 3.9 Hz), 141.4, 135.6 (q, *J* = 3.6 Hz), 130.3 (q, *J* = 34.0 Hz), 128.6, 128.5, 126.2, 124.6, 122.5 (q, *J* = 273.1 Hz), 67.9, 40.1, 33.2, 30.7, 20.6; IR (thin film) 3394 (br), 3063 (w), 3028 (w), 2939 (m), 2862 (w), 1670 (s), 1531 (s), 1327 (s) cm^{-1}; LRMS (ESI, % base peak) *m/z* 453.1 (2, $[MK]^+$), 437.1 (57, $[MNa]^+$), 415.1 (100, $[MH]^+$), 351.2 (10), 334.0 (4), 312.1 (8), 280.0 (33); HRMS (ESI) *m/z* calc'd. for $C_{19}H_{22}F_3N_2O_3S$ $[MH]^+$ 415.1297, found 415.1296.

REFERENCES

Bewley, M.C., Graziano, V., Griffin, K., and Flanagan, J.M. (2006). The asymmetry in the mature amino-terminus of ClpP facilitates a local symmetry match in ClpAP and ClpXP complexes. J Struct Biol *153*, 113-128.

Guha, R., Howard, M.T., Hutchison, G.R., Murray-Rust, P., Rzepa, H., Steinbeck, C., Wegner, J.r., and Willighagen, E.L. (2006). The Blue ObeliskInteroperability in Chemical Informatics. Journal of Chemical Information and Modeling *46*, 991-998.

Kuntz, I.D., Blaney, J.M., Oatley, S.J., Langridge, R., and Ferrin, T.E. (1982). A geometric approach to macromolecule-ligand interactions. J Mol Biol *161*, 269-288.

Lang, P.T., Brozell, S.R., Mukherjee, S., Pettersen, E.F., Meng, E.C., Thomas, V., Rizzo, R.C., Case, D.A., James, T.L., and Kuntz, I.D. (2009). DOCK 6: combining techniques to model RNA-small molecule complexes. RNA *15*, 1219-1230.

Laue, T.M., Shah, B.D., Ridgeway, T.M., and Pelletier, S.L. (1992). Computer-aided interpretation of analytical sedimentation data for proteins. In Analytical ultracentrifugation in biochemistry and polymer science, S.E.H.e. al., ed. (Cambridge, UK, The Royal Society of Chemistry), pp. 90-125.

Lo, J.H., Baker, T.A., and Sauer, R.T. (2001). Characterization of the N-terminal repeat domain of *Escherichia coli* ClpA-A class I Clp/HSP100 ATPase. Protein Sci *10*, 551-559.

Michel, K.H., and Kastner, R.E. (1985). A54556 antibiotics and process for production thereof. (US Patent 4492650).

Schuck, P. (2000). Size-Distribution Analysis of Macromolecules by Sedimentation Velocity Ultracentrifugation and Lamm Equation Modeling. Biophys J *78*, 1606-1619.

Wang, Y., Xiao, J., Suzek, T.O., Zhang, J., Wang, J., and Bryant, S.H. (2009). PubChem: a public information system for analyzing bioactivities of small molecules. Nucl Acids Res *37*, W623-633.

interactions. Specifically, CASK is known to interact with ZO1, which interacts with JAM2, which interacts with Pard3, thus bringing CASK and Pard3 into proximity. However, the work presented here shows that CASK and Pard3 interact directly through dimerization of their PDZ domains. Why these two proteins interact directly requires further investigation, but now that Chang et al. (2011) have identified every PDZ-PDZ interaction from the mouse proteome, they have paved the way for establishing the biological significance of these interactions.

REFERENCES

Chang, B.H., Gujral, T.S., Karp, E.S., BuKhalid, R., Grantcharova, V.P., and MacBeath, G. (2011). Chem. Biol. *18*, this issue, 1143–1152.

Hartwell, L.H., Hopfield, J.J., Leibler, S., and Murray, A.W. (1999). Nature *402* (6761, Suppl), C47–C52.

Heyduk, T., Ma, Y., Tang, H., and Ebright, R.H. (1996). Methods Enzymol. *274*, 492–503.

Hillier, B.J., Christopherson, K.S., Prehoda, K.E., Bredt, D.S., and Lim, W.A. (1999). Science *284*, 812–815.

MacBeath, G., and Schreiber, S.L. (2000). Science *289*, 1760–1763.

Oda, K., Matsuoka, Y., Funahashi, A., and Kitano, H. (2005). Mol. Syst. Biol. *1*, 2005.0010.

Songyang, Z., Fanning, A.S., Fu, C., Xu, J., Marfatia, S.M., Chishti, A.H., Crompton, A., Chan, A.C., Anderson, J.M., and Cantley, L.C. (1997). Science *275*, 73–77.

Chemical Activators of ClpP: Turning Jekyll into Hyde

David A. Dougan[1,*]
[1]Department of Biochemistry, La Trobe Institute for Molecular Science, La Trobe University, Melbourne 3086, Australia
*Correspondence: d.dougan@latrobe.edu.au
DOI 10.1016/j.chembiol.2011.09.003

Casein lytic peptidase P (ClpP) is a serine peptidase that, when coupled to its cognate ATPase, facilitates the controlled degradation of both damaged and unwanted proteins in bacteria. In this issue of *Chemistry & Biology*, Leung et al. (2011) report a small molecule screen against ClpP, from which they identified four structurally distinct compounds that activate ClpP for unregulated proteolysis.

The treatment of bacterial infections with antimicrobial drugs was one of the most profound medical advances of the last century. The discovery of these drugs began in the 1930s and continued unabated over the next four decades. Indeed, many of the drugs we use today can be traced back to natural compounds, identified during these "golden" years of drug discovery, and their effectiveness is evidenced by our current quality of life. However, since the end of this fruitful period of drug discovery, relatively few new compounds (natural or synthetic) have been developed. Concomitantly, especially during the last decade, there has been a concerning increase in the occurrence of nosocomial infections involving drug resistant bacterial species (e.g., Methicillin-resistant *Staphylococcus aureus* [MRSA] and Vancomycin-resistant *Enterococci* [VRE]) (Levy and Marshall, 2004) that has in turn lead to the emergence of multi-drug resistant (MDR) bacteria. Hence, there is a real need for the development of new drugs, especially those that target novel mechanisms to kill bacterial cells.

In 2005, Brötz-Oesterhelt and colleagues identified a new class of natural antibiotics termed acyldepsipeptides (ADEPs) that showed remarkable promise, as they were active in the treatment of rodents infected with antibiotic resistant bacteria (Brötz-Oesterhelt et al., 2005). Surprisingly, these compounds do not kill bacteria by inhibiting an essential cellular process, but rather they target a non essential protein, the peptidase ClpP, to kill bacteria. Indeed ADEPs are proposed to kill bacteria via a unique mechanism—by triggering the widespread and unregulated degradation of nascent polypeptides and unfolded proteins (Kirstein et al., 2009). Despite their remarkable bactericidal activity, limited availability of these antibiotics has hampered progress in elucidating their mechanism of action; hence the identification of new ClpP activators of unregulated proteolysis may aid in further defining how this promising class of drug functions.

ClpP is a barrel-shaped protein composed of two heptameric rings in which the catalytic residues are sequestered inside a proteolytic chamber. In the absence of its cognate AAA+ (ATPase associated with various cellular activities) component (e.g., ClpA, ClpC or ClpX), entry into this chamber is restricted to a narrow entry portal at either end of the complex (Wang et al., 1997). In this state, although short peptides can enter the proteolytic chamber for hydrolysis, large polypeptides are generally excluded from the chamber, preventing the indiscriminate degradation of cellular proteins. Therefore, in the absence of its cognate ATPase, protein degradation by ClpP is effectively turned OFF (Figure 1). By contrast, in the presence of its cognate ATPase, ClpP-mediated protein degradation is turned ON (Figure 1). Currently, it is widely accepted that activation of ClpP results from docking of a specific loop (known as the IGF loop) on the cognate ATPase (Kim et al., 2001), which culminates in opening of the narrow entry portal located at the distal ends of the complex, supporting entry of unfolded polypeptides, into the proteolytic chamber (Burton et al., 2001).

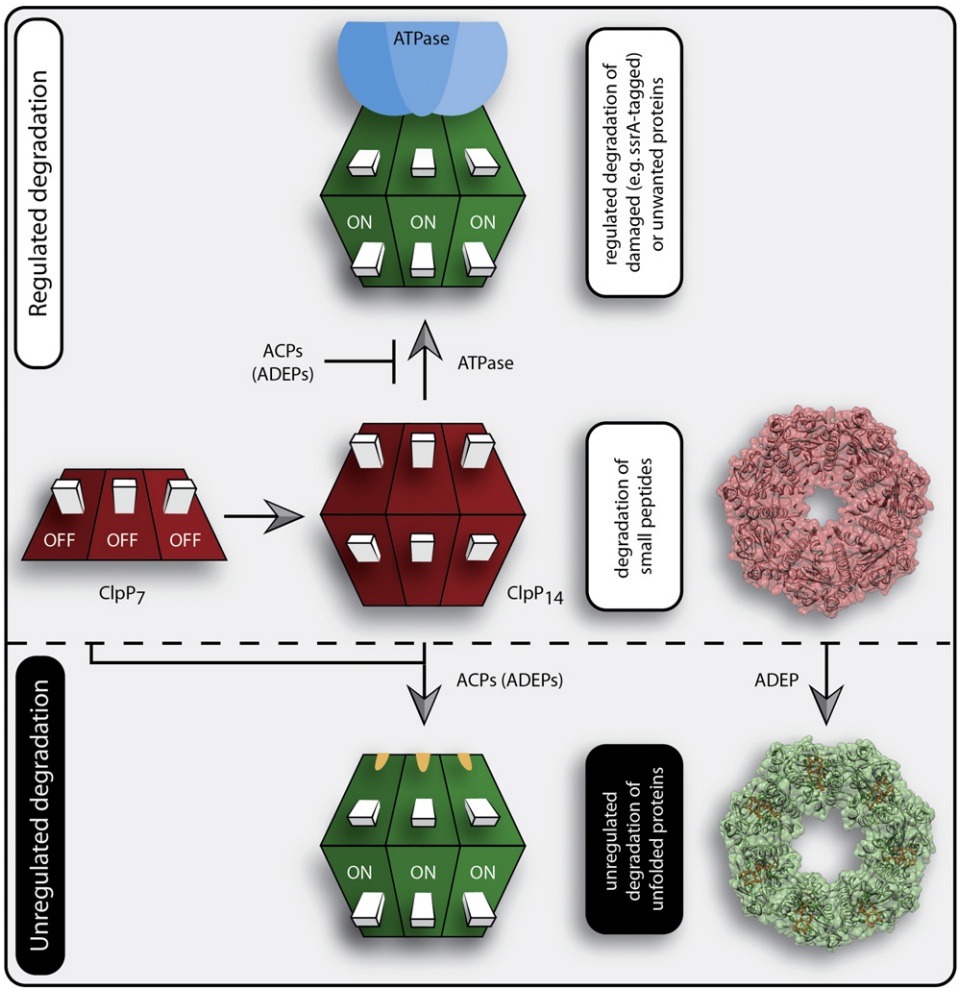

Figure 1. Activators of Self-Compartmentalizing Proteases Turn ClpP On for "Unregulated" Proteolysis
ClpP-mediated protein degradation is normally a highly regulated process in bacteria. Under normal conditions, the degradation of large protein substrates by single- or double-ringed oligomers of ClpP is effectively turned OFF (red) and only small peptides can access the catalytic residues located inside the proteolytic chamber. Consistently, the pore of ClpP is "closed," diameter of ~10 Å (red ring, left side). However, in the presence of its cognate ATPase (blue), ClpP is turned ON (green) and the regulated degradation of selected substrates (e.g., SsrA-tagged proteins) can proceed. The SsrA tag is an 11 amino acid motif, attached to the C terminus of "stalled" translation products in bacteria, that is essential for ATPase-mediated recognition of these incomplete proteins. By contrast, ACPs and ADEPs (yellow) activate ClpP for unregulated protein degradation by opening the pore to a diameter ~20 Å (green ring, right side), permitting the entry of large unfolded proteins into the catalytic chamber of ClpP in the absence of its cognate ATPase component.

In the current study, Leung et al. (2011) exploit the idea that ClpP is a useful drug target and have developed a simple fluorescence-based assay to identify small molecules that activate ClpP for ATPase-independent or "unregulated" degradation of large polypeptides. Specifically, they employed a high-throughput screen to monitor the ClpP-mediated degradation of a fluorescently labeled model "unfolded" protein (Fluorescein isothiocyanate labeled casein or FITC-casein). In the absence of ClpP activation, FITC-casein is stable, and hence the fluorescence signal is quenched; however upon activation of ClpP, FITC-casein is degraded into short FITC-labeled peptides, which are highly fluorescent. Using this assay, the authors screened approximately 60,000 small molecules from which they identified five new compounds (belonging to four different structural classes), called activators of self-compartmentalizing proteases (ACPs; ACP1–ACP5). Importantly, all five compounds were able to trigger the nonspecific degradation of several "unfolded" proteins; however, some compounds were considered better ClpP activators than others, as they were able to trigger the degradation of a broader range of substrates. From these five compounds, the best activator of ClpP - ACP1 (which was also considered to display good drug-like characteristics) was chosen for optimization and over 70 new derivatives were created, one of which (ACP1b) exhibited dramatically improved binding characteristics and activation qualities when compared to the parent compound.

Using a variety of biophysical techniques, the authors revealed that ACPs, like their natural cousins (ADEPs), activate ClpP through stabilization of the tetradecamer (Figure 1). Indeed, there was a good correlation between the binding affinity of the compound, stabilization of the double-ringed oligomer and activation of ClpP.

Also, through a combination of molecular docking simulations and biochemical experiments using various ClpP mutant proteins, the authors proposed that ACPs target two pockets on the surface of ClpP. Strong ACPs (e.g., ACP1b) bind exclusively to a hydrophobic pocket (H-pocket) located on the apical surface of ClpP, while weak ACPs (e.g., ACP2) appear to bind to both the H-pocket and a second pocket called the C-pocket (as it contains several charged residues), which is formed by the interface of two adjacent subunits in the heptameric ring. Consistent with an important role for the H-pocket in ClpP activation, recent structural analysis of ClpP in complex with ADEP (Lee et al., 2010; Li et al., 2010) revealed that ADEPs dock into the H-pocket, causing a conformational change in ClpP that triggers a dramatic opening of the entry portal into the proteolytic chamber (see Figure 1, right side). Interestingly, the ClpP activators (that bind exclusively to the H-pocket) not only trigger unregulated degradation of unfolded proteins in the absence of the cognate ATPase, but also inhibit the tightly regulated degradation of a model SsrA-tagged protein (i.e., GFP-ssrA), which represents an ATPase-dependent substrate. Collectively, these findings suggest that chemical activators of ClpP, such as ACPs and ADEPs, may function as IGF-loop mimetics, and hence these compounds may prove useful, not only in the development of future antimicrobial drugs but also in providing useful mechanistic insights into how ATPase(s) activate ClpP for degradation. Indeed this work reinforces the utility of ClpP as a potential drug target and provides a number of new structural frameworks from which potentially useful ClpP activators could be further developed into antibacterial drugs. Nevertheless, given that ClpP is also expressed in mammalian mitochondria where it is proposed to play an important role in the mitochondrial specific unfolded protein response, one may need to be cautious about the use of antibacterial drugs that target ClpP until the effect of these drugs has been studied on human ClpP and mitochondrial function. Alternatively, drugs that target HslV (a bacterial self-compartmentalized protease that is absent in higher eukaryotes) for unregulated degradation may have great promise.

ACKNOWLEDGMENTS

The author wishes to thank Kursad Turgay and Kaye Truscott for their helpful comments on the manuscript. D.A.D. is an Australian Research Fellow and work in his laboratory is supported by the Australian Research Council.

REFERENCES

Brötz-Oesterhelt, H., Beyer, D., Kroll, H.P., Endermann, R., Ladel, C., Schroeder, W., Hinzen, B., Raddatz, S., Paulsen, H., Henninger, K., et al. (2005). Nat. Med. *11*, 1082–1087.

Burton, R.E., Siddiqui, S.M., Kim, Y.I., Baker, T.A., and Sauer, R.T. (2001). EMBO J. *20*, 3092–3100.

Kim, Y.I., Levchenko, I., Fraczkowska, K., Woodruff, R.V., Sauer, R.T., and Baker, T.A. (2001). Nat. Struct. Biol. *8*, 230–233.

Kirstein, J., Hoffmann, A., Lilie, H., Schmidt, R., Rubsamen-Waigmann, H., Brotz-Oesterhelt, H., Mogk, A., and Turgay, K. (2009). Mol. Med. *1*, 37–49.

Lee, B.G., Park, E.Y., Lee, K.E., Jeon, H., Sung, K.H., Paulsen, H., Rübsamen-Schaeff, H., Brötz-Oesterhelt, H., and Song, H.K. (2010). Nat. Struct. Mol. Biol. *17*, 471–478.

Leung, E., Datti, A., Cossette, M., Goodreid, J., McCaw, S.E., Mah, M., Nakhamchik, A., Ogata, K., El Bakkouri, M., Cheng, Y.-Q., et al. (2011). Chem. Biol. *18*, this issue, 1167–1178.

Levy, S.B., and Marshall, B. (2004). Nat. Med. ***10*** (12, Suppl), S122–S129.

Li, D.H., Chung, Y.S., Gloyd, M., Joseph, E., Ghirlando, R., Wright, G.D., Cheng, Y.Q., Maurizi, M.R., Guarné, A., and Ortega, J. (2010). Chem. Biol. *17*, 959–969.

Wang, J., Hartling, J.A., and Flanagan, J.M. (1997). Cell *91*, 447–456.

This week in therapeutics

Indication	Target/marker/pathway	Summary	Licensing status	Publication and contact information
Infectious disease				
Bacterial infection	ATP-dependent Clp protease proteolytic subunit (clpP)	*In vitro* studies identified clpP activators that could help treat bacterial infections. In a high throughput screen for *Escherichia coli* clpP activators, 5 compounds were identified that promoted clpP-mediated protein degradation activity *in vitro* and had bactericidal activity against a panel of 10 bacterial species. The most drug-like compound, termed ACP1 (activator of self compartmentalizing protease 1), was optimized to increase bactericidal activity. Next steps include further optimization of the activators for animal models of bacterial infection. *SciBX* 4(40); doi:10.1038/scibx.2011.1119 Published online Oct. 13, 2011	U.S. provisional patent application filed; available for licensing worldwide	Leung, E. *et al. Chem. Biol.*; published online Sept. 23, 2011; doi:10.1016/j.chembiol.2011.07.023 **Contact:** Walid A. Houry, University of Toronto, Toronto, Ontario, Canada e-mail: walid.houry@utoronto.ca